TAJKARIMI, MEHRDAD, Ph.D. Experimental Evolution of Silver Nanoparticle Resistance in *Escherichia coli* (2015)
Directed by Dr. James G. Ryan 91 pp

The recent exponential increase in the use of engineered nanoparticles (eNPs) means both greater intentional and unintentional exposure of eNPs to microbes. Intentional use includes the use of eNPs as biocides; unintentional exposure results from the fact that eNPs are included in a variety of commercial products (paints, sunscreens, cosmetics.) Many of these eNPs include heavy metals or metal oxides such as titanium dioxide, silver, gold, zinc and zinc oxide. The fact that early studies of the impact of metallic nanoparticles achieved approximately 90% lethality to Ag, Cu eNPs, suggests that genetic variants are already circulating in bacteria that can be co-opted to provide heavy metal eNP resistance. This project has utilized laboratory experimental evolution to evolve eNP resistance in the bacterium *Escherichia coli* (K12 MG1655 strain.). This is currently being validated by demonstrating the greater fitness of evolved strains versus ancestral strains in the presence of different sized and coated silver nanoparticles (10nm, 40nm, citrate-coated, PVP-coated) as well as phenotypic changes in the bacterial cell wall (as measured by Atomic Force Microscopy, AFM.). Finally, the bacterial genomes of the evolved and ancestral strains were resequenced. The genomic basis of this complex phenotype was determined. The practical application of such knowledge cannot be underestimated since nature is already evolving nanoparticle resistant bacteria. Thus knowledge of the nature of the physiological, morphological, and genomic mechanisms of resistance will be essential to deploy sustainable use of NPs as biocides, and to prevent unintentional environmental damage.

EXPERIMENTAL EVOLUTION OF SILVER NANOPARTICLE RESISTANCE IN *ESCHERICHIA COLI*

by

Mehrdad Tajkarimi

A Dissertation Submitted to
the Faculty of The Graduate School at
The University of North Carolina at Greensboro
in Partial Fulfillment
of the Requirements for the Degree
Doctor of Philosophy

Greensboro
2015

Approved by

_____
Committee Chair

This work dedicated to my wife, Rashin and my son, Ali

APPROVAL PAGE

This dissertation has been approved by the following committee of the Faculty of The Graduate School at The University of North Carolina at Greensboro.

Committee Chair James G. Ryan PhD

Committee Members Joseph L. Graves Jr. PhD

Dennis R. LaJeunesse PhD

Ethan W. Taylor PhD

Albert M. Hung PhD

09/30/2014
Date of Acceptance by Committee

09/30/2014
Date of Final Oral Examination

ACKNOWLEDGEMENTS

During my almost 4 years of experience as a PhD student for second time, I found this long journey a fascinating experience. I am grateful to my advisor Dr. Joseph L. Graves as well as my mentor Dr. James G. Ryan. It has been honor to be your Ph.D. student, and I do appreciate all your valuable contributions to simulate and support my doctoral project. Despite having some obstacles during my first year of research, I find that being a mentor is more valuable and admirable than being a scientist.

I should also mention one of my best mentors, friend and supporter Professor Dean O. Cliver. He was a great scientist and encouraged me during my starting career in the US. I missed him and I always admire him.

I owe special thanks to Dr. Dennis LaJeunesse, who always share his precious comments along with positive energy and support in the lab.

I am very grateful and thankful for Dr. Albert Hung; he is one of the few mentors who was a key for my success that probably will be very important aspect of my future research in the field of nanotechnology. His patience and support always helped me to have a positive contribution in my research.

Dr. Ethan Taylor is one of my best professional supporters in my career by his valuable and insightful comments on my work an effective scientist in community.

I would like to thank my wife Rashin Sedighi for her love and encouragement and support when I needed it the most. I also would like to thank my son, Ali for all the years that he was patience with my ling education period that he was very important part of all

of my educations from my long educational journey from 2000-2014; First PhD, first post doctorate, Masters, second post doctorate and finally this second PhD. Thank you both of you with all my heart.

TABLE OF CONTENTS

Page

LIST OF TABLES

Page

LIST OF FIGURES

Page

CHAPTER I

INTRODUCTION

Emerging outbreaks of infectious disease and widespread resistance to conventional antimicrobial drugs are significant global public health problems, and there has been an increasingly aggressive search for new antimicrobial agents (Jones et al., 2008; M. Rai, Yadav, & Gade, 2009). Antibiotic resistant organisms that are causing dangerously untreatable clinical infections is a growing global and national problem for human and agricultural health (Chait, Vetsigian, & Kishony, 2012). Furthermore, resistance can be horizontally transmitted to other hosts accelerating the epidemic spread of antibiotic-resistant infections (Bonhoeffer, Lipsitch, & Levin, 1997). Thus drug resistant organisms are rapidly spreading inside hospitals, healthcare settings, food and water sources as well as in the community. When treatment failure happens, second or third choice drugs may be required that might be less effective, more toxic, and more expensive (CDC, 2012; Nelson DuránI, 2010). Maintaining the efficacy of existing antibiotics is reasonable strategy in the current conditions. This is because the rate of new drug discovery is slow and the fact that microbes are constantly evolving resistance to those that are developed (Chait et al., 2012).

For the reasons above, metallic and metallic oxide nanoparticles are being proposed as the new "miracle" antibiotics (Rai et al. 2012.) Silver nanoparticles have

been extensively employed as antimicrobials (Rai, Yadav, and Gade 2009). Silver have been used for its medical and antimicrobial effects from the ancient Romans to the water treatment systems in to the Apollo, MIR and the Space shuttle programs.(Prabhu & Poulose, 2012; R. S. Rai & Subramanian, 2009; Silver & Phung, 2005; Xiu, Zhang, Puppala, Colvin, & Alvarez, 2012). Past examples of the antimicrobial use of silver include its use for water treatment in 1000 BCE, the use of silver nitrate to treat venereal disease in 1700 CE, and the use of silver nitrate to treat fresh burns from at least the 18th century forward (Castellano et al., 2007; Prabhu & Poulose, 2012; R. S. Rai & Subramanian, 2009; Xiu et al., 2012). In addition, various types of silver compounds with nitrate, sulfadiazine, zeolite, powder, oxide, chloride and silver cadmium powder have been used as antimicrobials from ancient times (M. K. Rai, Deshmukh, Ingle, & Gade, 2012). In modern times, silver has been successfully used as an antimicrobial. For example, Spadaro et al. (1974) utilized silver electrodes with weak direct current to inhibit the growth on agar plates of *Staphylococcus aureus*, *Escherichia coli*, *Proteus vulgaris*, and *Pseudomonas aeruginosa*. Also a recent study showed silver effective against 16 major species of bacteria (Prabhu & Poulose, 2012).

1.1 Nanoparticle Characteristics and their Impact on Microbes

Nanoparticles have been proposed to be effectiveness antimicrobials due to their high surface-to-volume ratio and their unique chemical and physical properties which are often best realized through the use of metallic compounds (Kim et al., 2007; Jose Ruben Morones et al., 2005; M. Rai et al., 2009). Sondi and Salopek-Sondi (2004) is one of the earliest studies that examined specifically the impact of silver nanoparticles (AgNP) on

bacterial growth (Sondi & Salopek-Sondi, 2004). Their study with *Escherichia coli* and 12 nm diameter nanoparticles suggested that if the primary mechanism of biocidal action is Ag+ ions, then AgNPs would be more effective than bulk silver. In all treatments (10, 50, and 100 $\mu g/cm^3$), there was a significant delay in bacterial growth and lower population size achieved at the end of 9 hours relative to the control (0 $\mu g/cm^3$). Sondi and Salopek-Sondi (2004) argued that this was because the concentration of the AgNPs decreased with time in the culture and interaction of the AgNPs with the intracellular substances of the destroyed cells. Their scanning electron microscope (SEM) images showed that AgNPs coagulated with dead bacterial cells, thus reducing the concentration of them and Ag+ ions in the liquid medium. Subsequent studies have confirmed these general findings (Baker, Pradhan, Pakstis, Pochan, & Shah, 2005; Jose Ruben Morones et al., 2005; Pal, Tak, & Song, 2007; Panáček et al., 2006; Shahverdi, Fakhimi, Shahverdi, & Minaian, 2007). These impacts of AgNPs have also been found for natural microbial communities (Burchardt et al., 2012; Merrifield et al., 2013).

Nanoparticle morphology (size, shape) is an important determinant of toxicity to bacteria with smaller NPs being most effective than larger NPs (Baker et al., 2005; Panáček et al., 2006). Morones et al. (2005) studied NPs in the range of 1 – 100 nm diameters and found that toxicity was enhanced based on a lower size range (1 – 10 nm), and observed a range of varying NP shapes through transmission electron microscopy (TEM; (Jose Ruben Morones et al., 2005). Pal et al. (2007) found that truncated triangular AgNPs displayed the greatest effect on *E. coli*, compared to spherical and rod-shaped NPs (Pal et al., 2007).

Nanoparticles are generally produced by spark discharging, electrochemical reduction, solution irradiation and cryochemical synthesis, and biological processes. The method by which the particle is produced has important impacts on its physicochemical properties, such as pH-dependent partitioning and biological activity, as compared to bulk material (Birla et al., 2009; M. K. Rai et al., 2012; Shahverdi et al., 2007; Sondi & Salopek-Sondi, 2004; Wu & Hsu, 2008). Chemical methods require some sort of compound coating the AgNPs to prevent further aggregation. For example, Sondi, Goia, and Metijevic` (2003) utilized Daxad 19, a sodium salt of high molecular weight naphthalene sulfonate formaldehyde to prevent NP aggregation (Sondi & Salopek-Sondi, 2004). Others have used citrate ($C_6H_5Na_3O_7$), thiosalicyclic acid (C_6H_4 (SH) CO2H, IUPAC name, 2-mercaptobenzoic acid), or polyvinylpyrrolidone (PVP, IUPAC name 1-ethenylpyrrolidin-z-one) as coating agents for AgNP production. The fact that these coatings have different solubility's would result in them impacting solution pH differently. This in turn may result in the NPs adhering to biological cell walls differently. This suggests that coating type may play a crucial role in how AgNPs kill bacteria. El Badaway et al. (2011) showed that toxicity of AgNPs was dependent on more negatively charged particle coating. In a study performed on *Bacillus* spp., they found toxicity increased along the following series of coatings: uncoated (H_2—AgNPs), citrate coated (Citrate-AgNPs), polyvinylpyrrolidone coated (PVP-AgNPs), and branched polyethyl-eneimine coated (BPEI-AgNPs) (El Badawy et al., 2011).

Schacht et al, 2013, briefly describe the mechanism of nanosphere Ag(0) silver nanoparticles in three steps 1) attachment of Ag(0) nanoparticles to the cell surface and

altering the physical, chemical, and functional properties of the cell membranes 2) adding more damage to bacterial cells by permeating the cell, DNA, proteins and other phosphorus- and sulfur-containing cell constituents interaction 3) silver ions release and generating an amplified size and dose dependent biocidal effect (Schacht et al., 2013).

The antimicrobial activity of silver has been established to be due to Ag+ ions in a number of studies going back at least to the 1970's(Mijnendonckx, Leys, Mahillon, Silver, & Van Houdt, 2013). Cell lysis or inhibition of cell transduction, interaction with thiol (-SH) groups of membrane-bound enzymes or proteins and effects on respiratory chain of bacteria has been acknowledged as sources of the antimicrobial effects of silver nanoparticles. Also AgNPs have lower relative therapeutic doses compare to other antimicrobials (Olesja Bondarenko, 2013; Prabhu & Poulose, 2012; Xiu et al., 2012) and it has been claimed that due to the fact AgNPs impact so many bacterial systems that there is a lower chance of developing antimicrobial resistance to them (Jain et al., 2009; Madhavan, Rosemary, Nandkumar, Krishnan, & Krishnan, 2011).

While the exact mechanisms of silver nanoparticle toxicity to bacteria are not fully known, there is a growing consensus concerning the candidate actions. For example, some studies have shown that the toxicity of AgNps can be influenced by adding functional groups to the particle (e.g. sulfidation reduces toxicity, Levard et al. 2013.) Bondarenko et al. 2013 found that cell NP contact increases the dissolution rate of Ag+ ions and hence their toxicity on six bacterial species (*E. coli, Pseudomonas flourescens, P. putida, P. aeruginosa, Bacillus subtilis, and Staphylococcus aureus*). First, the action of silver nanoparticles occurs both by the release of silver ion (Ag+) as well as from

potential disruption or damage to the cell wall and membrane caused by the particles themselves(Mijnendonckx et al., 2013; M. Rai et al., 2009; M. K. Rai et al., 2012). Silver interacts with the thiol group compounds found in respiratory enzymes of bacterial cells. It also binds to the bacterial cell wall and cell membrane inhibiting the respiration process (Klasen, 2000; M. Rai et al., 2009).

Silver is known to act on *E. coli* by inhibiting the uptake of phosphorous and releasing phosphate, mannitol, succinate, proline, and glutamine from the cells (M. K. Rai et al., 2012; Yamanaka, Hara, & Kudo, 2005). The penetration of silver ions inside the cell is thought to impact the ability of DNA to replicate by causing it to condense. Due to the large surface area to volume ratio, smaller AgNPs should be able to more effectively release Ag+ ions into the cell and, following attachment to the cell membrane, may also penetrate into the cell (Mijnendonckx et al., 2013; Jose Ruben Morones et al., 2005; Pal et al., 2007; M. K. Rai et al., 2012). Once inside, Ag+ ions may be lethal as they disrupt metabolism, cell signaling, DNA replication, transcription, translation, and cell division, either directly or through the generation of reactive oxygen species (ROS)(Mijnendonckx et al., 2013; M. K. Rai et al., 2012).

Silver resistance bacteria were repeatedly found in burn wounds, clinical and natural environments, teeth. In all *E. coli* strains, cus CFBARS determinants in chromosomally located area partly caused by single point mutation that are functioning to develop, Ag+ binding proteins, ATPase efflux pump, spans the entire cell membrane and pumping Ag+ from the periplasm to the exterior of the cell. Lack of this determinant can take about 100 times more sensitive strain(Mijnendonckx et al., 2013). In summary, the

toxicity of AgNPs upon bacteria appears dependent on particle shape, size, and concentration (> 75 ug/ml usually ceases growth(M. K. Rai et al., 2012). The toxicity of AgNPs is determined by the dissolution rate. In addition the toxicity of AgNPs differed widely between six species of bacteria tested (gram positive and gram negative; (Martinez & Baquero, 2000; Olesja Bondarenko, 2013).

Moreover, it has been shown that the morphological properties of AgNPs have indirect effects on the release of Ag+ ions. Thus AgNP antimicrobial activity is a combination of oxygen availability, particle size, shape, and/or type of coating, aggregated state, stability of the preparation, dosage and speciation of the released silver (Burchardt et al., 2012; Wilkinson, White, & Chipman, 2011; Xiu et al., 2012). This study tests the generality of these results by specifically comparing two different commonly used coatings (citrate, PVP) and examine toxicity for 10 nm and 40-nm AgNPs in the model gram-negative bacterium *Escherichia coli*.

1.2 Nanoparticles and the Environment

Increasing amounts of metallic/metallic oxide nanoparticles are being used in consumer products. For example, nano-TiO_2 is produced on a large scale for applications in paints, cosmetics, sunscreens, photocatalysts and solar cells, as well as water purification devices (Mu and Sprando 2010; Planchon et al. 2013.) In 2008 the concentration of nano-TiO_2 predicted for American soil, sludge, surface water, sewage treatment plant (STP) effluent, STP sludge, and sediment were 0.53 mg/kg/year, 42.00 mg/kg/year, 0.002 mg/L/year; 1.75 mg/L/year; 137 mg/kg/year, and 53 mg/kg/year, respectively (Gottschalk et al. 2009.) Similarly values for nano-Ag were calculated at

6.6 mg/kg/year, 526 mg/kg/year, 0.088 mg/L/year, 16.40 mg/L/year, 1.29 mg/kg/year, and 153 mg/kg/year, respectively.

In addition there are increasing concentrations of metals entering natural environments e.g. wastewater effluents (e.g. industry, hospitals, dental offices, etc.) and water flow from metal mines over the last decade. Therefore there is great potential for environmental and agricultural damage caused by silver nanoparticles due to rapidly increasing quantities and varieties of this antimicrobial (Bradford, Handy, Readman, Atfield, & Muhling, 2009; Dobias & Bernier-Latmani, 2013; Jain et al., 2009; Martinez & Baquero, 2000; Reinsch et al., 2012; Schwab, 2012; Z. Zhang, Kong, Vardhanabhuti, Mustapha, & Lin, 2012) and widespread and uncontrolled use of silver may cause more bacterial resistance (Gupta & Silver, 1998). Already considerable modification in the structure and function of microbial communities has been caused by introduction of various forms of heavy metals such as Zn, Cu, Cr, Mn and Hg and Ag that some of them even have nutritional values (Bednorz et al., 2013; Hacioglu & Tosunoglu, 2014; Silva et al., 2012). In addition increased metal concentration may cause greater dissemination of mobile genetic elements and novel phenotypes among bacterial populations (Mijnendonckx et al., 2013).

The idea that increased use of silver as a biocide will generate novel phenotypes is evidenced from silver resistant bacterial strains isolated from patients in the Veterans Administration Hospital in Syracuse, NY. Strains living in hospitals have been exposed to a number of biocides and in general should be “tougher” than stains living in the general environment. Indeed, silver-resistant bacteria have been repeatedly found in burn

wards, clinical and natural environments, and on human teeth (Toprak et al., 2012). It has been shown that improper waste water treatment and fail to remove bio- pollutants are causing the contamination of surrounding environment and created a favorite habitat for emergence of new pathogens, containing new resistance and virulence genes and may facilitate their persistence, co-selection, and dissemination (Gomez-Sanz et al., 2013; Hacioglu & Tosunoglu, 2014; Varela & Manaia, 2013).

Considerable modification in the structure and function of microbial communities has been caused by introduction of various forms of heavy metals such as Zn, Cu, Cr, Mn and Hg and Ag that some of them even have nutritional values (Bednorz et al., 2013; Hacioglu & Tosunoglu, 2014; Silva et al., 2012). However, the presence of have metals such as chrome, nickel and mercury might have counter-selective effects against antimicrobial resistant strains against *E. coli* strains (Holzel et al., 2012).

1.3 Potential For NP Resistance

The chief mechanism of evolution is natural selection. For natural selection to operate a population must be variable, the trait in question must be heritable, and there must be a struggle for existence. We know that the mutation rate per bacterial nucleotide ranges between 10^{-7} to 10^{-10} (Ford et al. 2011; Ycart and Veziris 2014). This translates to a mutation rate per genome at about 10^{-1} to 10^{-3}. Indeed, the mutation rate per genome for *E. coli* K12 MG1655 (the bacterium used in these experiments) is around 0.87 – 1.51 x 10^{-3} per genome (Lee et al. 2012.) This means that since bacteria maintain large populations there are an ample number of mutations to allow bacterial evolution to proceed quickly.

Since mutations are changes in the genetic code they are passed on to the mutant's daughter cells. While most mutations are deleterious; a significant fraction are neutral, and an even smaller fraction that are beneficial. Beneficial mutations may rapidly sweep to high frequency when they confer an advantage against environmental toxins such as antibiotics or heavy metals (Levin, Perrot, Walker 1999; Miller, O'Neill, Chopra 2002; Burke 2012). Given what we already know about bacterial evolution, it seems contradictory that researchers developing new applications of metallic/metallic oxides for bacterial control have not considered if and how quickly resistance to these nanomaterials will evolve (Graves 2014.).

We already have the experience of the rapid bacterial evolution of resistance to traditional antibiotics (Baquero and Blazquez 1997; Levin, Perrot, and Walker (2000.) Over forty years ago, *Streptococcus pneumoniae* was considered widely susceptible to penicillin and other β-lactam antibiotics. Shortly afterwards, resistance to these antibiotics was reported all over the world, such that by 1997 resistance rates exceeded 30—70% of isolates derived from patients (Baquero and Blazquez 1997). Thus, understanding the mechanisms of evolution we should expect that despite the fact that metallic/metallic oxides NPs impact a great number of bacterial systems that the evolution of resistance to them is already occurring in nature.

Resistant genotypes seem to have lower growth rates than their sensitive counterparts in the absence of antimicrobials(Lenski, 1998). The mechanism of most bacterial heavy metal resistance results from energy-dependent ion efflux from the cell by membrane proteins that function either as ATPases or as chemiosmosis cation/proton

antiporters (Silver, 2003). The fact that these resistance mechanisms are already circulating in nature suggests that even naïve bacteria could acquire resistance in due to horizontal gene transfer. This could occur from food ingestion or inside gastrointestinal system (Durso, Miller, & Wienhold, 2012) resulting from sequential accumulation of multiple beneficial mutations or a single amino acid exchange (Tyerman, Ponciano, Joyce, Forney, & Harmon, 2013).

Single amino acid substitution has more advantage and could create rapid fixation within hundreds of generations in the presence of antibiotics (Tyerman et al., 2013). Spontaneous mutation is an important source of variation driving the evolution of resistance, however, developing strong resistance requires multiple mutations for most antimicrobials (Toprak et al., 2012). It is also not clear how the evolution of biofilm formation contributes to the development of antimicrobial resistance (Tyerman et al., 2013). Moreover, our lack of understanding of the morphological and genomic changes of bacteria via natural selection at sub-lethal levels of silver nanoparticles will result in unforeseen problems such as the rapid emergence of silver nanoparticle resistance (Furuya & Lowy, 2006).

In addition to de novo evolution of silver nanoparticle resistance we can expect that existing silver resistance genetic elements will be co-opted by bacteria in nature to survive elevated silver concentrations. For example, the R- Plasmid is known to be one of the most common transmissible instruments for resistance through conjugation and transformation (Shoeb et al., 2012). In addition, a silver resistance plasmid of the IncHI

incompatibility group confers resistance to silver, mercury, tellurium, as well as several antibiotics (Gupta et al. 1999.)

This study avoids the complication of plasmid borne resistance by using *E. coli* K12 MG1655 a strain that has no plasmids. Table 1 show a list of existing antimicrobial resistance genes that are carried by *E. coli* (Furuya & Lowy, 2006). However, we do not have a-priori knowledge of how genomic variation will combine to produce resistance to silver nanoparticles in this particular strain of the bacterium. Whole-genome studies are beginning to demonstrate that the naïve "candidate" gene approach is simply inadequate to predict genomic evolution under different environments (e.g. Graves et al. in prep). In this study, Illumina resequencing via the MiSeq platform was used to determine which genomics variants were associated with evolved silver nanoparticle resistance. This allows comparsions of the resistance elements that evolved in this bacterial strain under our culture conditions, with previously scored resistance elements (e.g. Silver 2003).

1.4 Molecular Genetics of Silver Resistance

Current genomic evidence suggests that the sil Ag (I) resistance system may have evolved from an earlier existent pco copper resistance system. *Salmonella spp*. and *E. coli* genomes contain six genes (silA through sil S) that produce products that are closely homologous to a gene cluster on the *Escherichia coli* genome renamed as agr A, agr B, agr C, agr R, agr S in *E. Coli* K-12 and *E. coli* O157:H7. SilS (a histidine- containing membrane ATP kinase 'sensor') and silR (a cytoplasmic DNA-binding activator 'responder' that contains an aspartate residue that is trans-phosphorylated from SilS) are two genes that are transcriptionally responsible for silver resistance systems. The plasmid

borne silver resistance gene silAB ORF96silCRS is closely homologous to chromosomal gene regions in *E. coli* K-12 and O157:H7. SilP belongs in the family of heavy metal resistance efflux ATP-ases. It is reported that a deletion of DNA in the middle of silP results in reduced silver resistance. It has also been shown that silP eflux ATPase pump for cations such as cadmium, zinc or copper provides cation binding for transport and its modulation which is not significant in Ag efflux pumping system and detail functional studies has not been developed (Silver, 2003).

CHAPTER II

EXPERIMENTAL EVOLUTION OF SILVER NANOPARTICLE RESISTANCE

Experimental evolution is defined as research in which populations are studied across multiple generations under defined and reproducible conditions either in the laboratory or in nature (Garland and Rose 2009.) In laboratory natural selection experiments some aspect of the environment of laboratory maintained organisms is altered; e.g. culture, medium, food, temperature, humidity, etc.) The methodology has been long used in evolutionary biology going back to the work of Th. Dozhansky in the 1940's. It's successes in elucidating the nature of adaptation to a wide variety of environmental features are many; including the iconic long term evolution experiments of the Lenski laboratory in *E. coli* (Lenski et al. 1991; Lenski and Travisano 1994). Recent successes of this method particularly relevant to bacterial adaptation include Herring et al. 2006 (demonstrating bacterial adaptation on the laboratory time scale); and Tenaillon et al. 2012 (utilized > 100 replicates lines to demonstrate adaptive convergence in *E. coli*.).

This study utilized the experimental evolution methodology of these previous *E. coli* experiments to examine the evolvability of silver nanoparticle resistance. It was designed to determine how quickly silver nanoparticle resistance could evolve in a previously non-resistant *E. coli* K12, MG1655, a strain that had no previously known silver resistance genetic (sil) elements. The control populations were maintained in

standard medium without the addition of AgNPs. Both control and treatment groupswere replicated five-fold. After transfer to found the next generation, the remainder of each replicate was frozen in -80^{o} for future analysis. The treatment populations were exposed to increasing concentrations of spherical 10nm citrate-coated AgNPs. The AgNPs were citrate-coated due to the need to prevent agglomeration of the particles. Citrate was chosen for this experiment due to the inability of citrate to be metabolized by *E. coli* (Blount et al. 2012). Our laboratory has studied the impact of two commonly used silver nanoparticle coating types (citrate and polyvinylpyrolidone, PVP) on bacteria (Tajkarimi et al. 2014.) Generally, we found that citrate-coated were more effective against *E. coli* K12 MG1655 than PVP-coated.

The selection protocol consisted of culturing *E. coli* K-12 MG1655 using Davis Minimal Broth (DMB, Difco^{TM}Sparks, MD) with dextrose 10% as a sole carbon source, enriched with thiamine hydrochloride 0.1% (Thiamine Hydrochloride, Fisher scientific, Fair Lawn, NJ) in 10 ml of total culture volume maintained in 50 ml Erlenmeyer flasks. The flasks were placed in a shaking incubator at 37^{o} C for 24 hours. Cultures were propagated by daily transfers of 0.1 ml of each culture into 9.9 ml of DMB. This method is called the serial transfer in liquid medium protocol (Rosenzweig and Sherlock 2009.) There are other methods that can be used for laboratory experiments in bacteria, including the serial transfer in solid medium, and the continuous medium (chemostat) method. These methods differ in a number of attributes. For example, serial transfer experiments always involve a series of reduction in population size compared to

chemostat experiments where this does not occur. Thus it is likely that some of the results reported in this study are related to the type of experimental protocol used. Therefore this experiment was not designed to be all inclusive of every potential environmental circumstance under which bacteria may be exposed to AgNPs but rather is designed to test the hypothesis that evolution to AgNPs is possible under some environmental conditions.

The toxicity of metallic/metallic oxide NPs upon bacteria appears dependent on particle composition, shape, size, coating, and concentration (AgNPs concentrations of > 75 mg/ml usually ceases growth; Rai et al. 2012; Tajkarimi et al. 2014). It was determined that minimal growth of *E. coli* K12 MG1655 was observed at 50 □g/l so this was chosen as the initial concentration for the evolution of resistance studies. As bacterial cultures showed evidence of growth (observed as turbid cultures by inspection) the concentration of AgNPs in the base cultures for the treatment group was increased (per schedule shown in Table 2.) The optical density measurements showed that under these conditions that the cultures grew from about 10^6 to about 10^8 bacteria per ml at the end of 24 hours, having undergone about 6.5 generations.

The fact that increasing concentrations of AgNPs were used made this a directional selection experiment. In directional selection the population mean of a trait is shifted to higher or lower values by exposing each succeeding generation to either a greater or lesser amount of specific environmental variable. To determine the concentration most favorable to begin the selection experiment the bacteria were

systematically exposed to the concentrations of 1 mg/l, 10 mg/l, 25 mg/l, 50 mg/l and 100 mg/l. These concentrations effectively wiped out bacterial growth compared to the control treatment (0 mg/l). Therefore the treatment concentrations were lowered to 50 µg/l, 100 µg/l, 250 µg/l, 500 µg/l, 750 µg/l and 1000 µg/l. The 50 µg/l concentration was chosen as the initial concentration for the resistance studies.

After 50 generations of bacterial growth at this concentration, the treatment populations were exposed to 100 µg/l. This concentration was maintained for another 90 generations. After this the selection concentration was increased to 125 µ/l. This concentration was carried out for 125 generations. After 45 generations of exposure at this concentration it was observed that several of treatment replicates were losing viability. To rescue these populations, all replicates were combined. Five new replicates were created by sampling from the mixed pool. These were propagated without selection for AgNP resistance for for an additional 40 generation before the new replicates were again exposed to another 80 generations of 125 µg/L AgNps.

After 45 generations of growth in the 125 µg/L, these replicates were combined to form a "cocktail" to assay their silver resistance relative to the controls (that were also cocktailed.) The cocktail protocol was used due to a shortage of labor and materials. Table 2 shows the schedule of exposure concentrations used in the selection protocol. After 140 generations the exposure for the selected cultures had increased by 250%.

CHAPTER III

GENOTYPING SILVER NANOPARTICLE RESISTANCE; ANTIMICROBIAL ASSAYS

3.1 What Are Antimicrobial Assays?

Antimicrobial assays evaluate the effectiveness of antimicrobials or certain procedures against bacteria , mold and yeasts (Bharitkar et al., 2014; Hajmeer et al., 2011; Salam A. Ibrahim, 2011; M. Tajkarimi & Ibrahim, 2011; M. Tajkarimi et al., 2008; M. M. Tajkarimi, Ibrahim, & Cliver, 2010; M. X. Zhang et al., 2014). Antimicrobial quantifications in most experiments are based on two protocols, MIC (Minimum Inhibitory concentration) and MBC (minimum bactericidal concentration), which is presumably greater than the MIC.

MIC is defined in different terms; some of them are ‘‘lowest concentration resulting in maintenance or reduction of inoculum’s viability,” ‘‘lowest concentration required for complete inhibition of test organism up to 48 hours incubation,” ‘‘lowest concentration inhibiting visible growth of test organism,” or ‘‘lowest concentration resulting in a significant decrease in inoculum’s viability (>90%).(M. M. Tajkarimi et al., 2010)” or” the lowest concentration of a particular substance needed to inhibit the growth of a certain population of bacteria”(Kedziora et al., 2013). MBC is defined as ‘‘concentration where 99.9% or more of the initial inoculum is killed” or ‘‘lowest concentration at which no growth is observed after sub-culturing into fresh broth.

(M. M. Tajkarimi et al., 2010). The MIC method is cited by most researchers, but some quote MBC as a measure of antibacterial performance. Several antimicrobial assays are currently being used; here is a brief description of some of them:

Dilution plating and colony forming units enumeration is one of the methods that could be used to investigate the efficiency of the antimicrobials (Singh, Shiha, & Kumar, 2014). Disc-diffusion method is an approved method by the Food and Drug Administration (FDA) as a standard for the National Committee for Clinical Laboratory Standards. This method is usually used for preliminary studies. In this method, a paper disc soaked with the antimicrobial is placed on the inoculated surface of an agar plate and the zone of microbial inhibition is measured. There are other antimicrobial test methods such as drop-agar-diffusion method, broth microdilution method and direct-contact technique in agar (M. M. Tajkarimi et al., 2010).

3.2 Materials and Methods for Antimicrobial Assays

3.2.1 Bacterial Culture

We cultured *E. coli* K-12 MG1655 using Davis Minimal Broth (DMB, Difco™Sparks, MD) with Dextrose 10% (Dextrose, Fisher Scientific, Fair Lawn, NJ) as a sole carbon source, enriched with thyamine hydrochloride 0.1% (Thyamin Hydrochloride, Fisher scientific, Fair Lawn, NJ) in 10 ml of total culture volume maintained in 50 ml Erlenmeyer flasks. The flasks were placed in a shaking incubator with temperature maintained at 37^{o} C for 24 hours. Cultures were propagated by daily transfers of 0.1 ml of each culture into 9.9 ml of DMB.

3.2.2 Measuring Bacterial Growth

Bacterial growth in BHI broth samples was assessed by measuring turbidity at 620 nm for hours 0, 3, 6, 12 and 24, using a 98-well plate Synergic Mx spectrophotometer (Biotek, VA USA) using clear polyester 98-well plates.

3.2.3 Bacterial Enumeration

Bacterial populations were determined by spread plating on DM agar. In this procedure, samples were withdrawn from inoculated samples at 0 and 24 h and were serially diluted in 0.1% peptone water. Appropriate dilutions were surface plated (100 µl) onto duplicate DMA plates.

3.2.4 Antimicrobials Susceptibility Tests

The antibiotic susceptibility test was performed using the standard disk diffusion method (Bauer, Kirby, Sherris, & Turck, 1966).

3.2.5 Disk Diffusion Assay

A 0.5 McFarland standard is equivalent to a bacterial suspension containing between 1 x 10^8 and 2 x 10^8 CFU/ml of *E. coli* cells. The total number of bacteria were adjusted to the 0.5 McFarland standard and spread on the agar DMA plate. Then disks including 30 µg chloramphenicol as a positive control were inserted into the agar plate and the results were measured after 24 hours of incubation of the plated cells at 37 C.

3.2.6 Broth Micro Dilution Method

Preparing bacteria:

Overnight culture prepared and adjusted by McFarland standard at 0.5 McFarland turbidity. This results in a suspension containing approximately between 1 to 2 x 10^8

CFU/ml. The absorbance at 625 nm should be 0.08 to 0.13 for the 0.5 McFarland standards. Within 15 minutes of preparation, the inoculum suspension is adjusted in water, saline, or broth. After inoculation the bacteria are diluted 10 times and 5 µl of the inoculum is added to each well. In this case, we have about 5 x 10^4 CFU/well. Next 50 µl of the MH broth is added to each well. We used 1mg/ml= 1g/L of the AgNPs and made systematic dilution series to find the proper antimicrobial concentration. The 12 dilution series were prepared as follows:

1. SOLUTION 1: 120 µl of 10nm citrate coated AgNPs (1mg/ml) were taken and added to 100 mg/l 1080 µl of DI water.
2. 500 µl of SOLUTION 1 is added to two centrifuge tubes labeled " C1 " and diluted with 500 µl of DI water
3. 350µl of SOLUTION 1 is added to two centrifuge tubes labeled " C2 " and diluted with 650 µl of DI water
4. 200 µl of SOLUTION 1 is added to eight centrifuge tubes labeled 20 mg/l "A" and diluted with 800 µl DI water
5. 250 µl of "A" is added to four centrifuge tubes labeled 5mg/l " D" and diluted with 750 µl DI water
6. 500 µl of "D " added to three centrifuge tubes labeled "G" and diluted with 500 µl DI water

3.2.7 Plate Process Column

1. After adjusting the culture with 0.5 McFarland standard it was diluted 10 times (50 µl of the adjusted culture was added and diluted with 45 µl of Broth). Then 95 µl of MH Broth x 5 µl of the stock culture was added.)
2. 50 µl of SOLUTION 1 and 45 µl of broth x 5 µl culture 50 mg/l
3. 50 µl of " C1 " and 45 µl of broth x 5 µl culture 25 mg/l
4. 50 µl of " C2 " and 45 µl of broth x 5 µl culture 17.5 mg/l
5. 50 µl of " A " and 45 µl of broth x 5 µl culture 10 mg/l
6. 37.5 µl of " A " and 57.5 µl of broth x 5 µl culture 7.5 mg/l
7. 25 µl of " A " and 70 µl broth x 5 µl culture 5 mg/l
8. 12.5 µl of " A " and 32.5 µl broth x 5 µl culture 2.5 mg/l
9. 25 µl of " D " and 70 µl broth x 5 µl culture 1.25 mg/l
10. 12.5 µl of " D " and 82.5 µl broth x 5 µl culture 625 µg/l
11. 6.25 µl of " D " and 88.75 µl broth x 5 µl culture 312 µg/l
12. 25 µl of "G" and 70 µl broth x 5 µl culture 156 µg/l

3.3. Visual Characterization Techniques

3.3.1 Electron Microscopy

Scanning Electron Microscopy bacterial preparation

SEM preparation was conducted using aldehyde fixative for a minimum of one hour using Karnovsky's glutaraldehyde, followed by 2% paraformaldehye/2% glutaraldehyde in 0.1M phosphate buffer for another hour, post-fixation with osmium

tetroxide and cacodylate phosphate buffer for one hour and washing with deionized water, followed by applying a series of graded acetonitrile using concentrations of 50, 70, 90, 95, and 100%. Images were generated using Zeiss Auriga BUFIBFE SEM.

3.3.2 Atomic Force Microscopy

In force spectroscopy, the AFM cantilever is moved in the z-direction and its position is recorded. The force acting on the cantilever movement is calculated as a spring constant and recorded by a force distant curve with pN (10^{12} N) sensitivity (Dufrene & Pelling, 2013). AFM has been used successfully in the following applications: submolecular-resolution imaging, *in situ* observation, and nanomechanics measurement(Zhong & He, 2012).

Lifshitz-Van der Waals adhesion forces play an important role in the adhesion of bacteria to various surfaces (Chen, Harapanahalli, Busscher, Norde, & van der Mei, 2014). Antimicrobial compounds, could disrupt the peptidoglycan layer and inhibit protein or DNA synthesis. These physiological changes to the bacterial physical properties, such as their elasticity and viscosity and measurement of these properties could provide important insights into the mechanism of action of antibiotic agents (Vadillo-Rodriguez, Beveridge, & Dutcher, 2008). Comprehensive understanding of interaction between bacterial cell surface and the related change in contact area is required to consider the viscoelasticity of the bacterial cell surface. The qualitative differentiation of bacterial viscoelastic properties has yet to be applied to studying bacterial biofilms (Nunez et al., 2005; Volle, Ferguson, Aidala, Spain, & Nunez, 2008). Understanding bacterial viscoelastic properties is becoming more important because it is

now believed that bacterial colonization and biofilm formation are intimately related to substrate adhesion forces. The ability of bacteria to persist in biofilms is plays a critical role in infectious disease (Childers, Van Laar, You, Clegg, & Leung, 2013; Haraguchi, Miura, Fujise, Hamachi, & Nishimura, 2014). Understanding the adherence mechanism to solid surfaces is an important step to understand the communal lifecycles of bacteria (Rogers, van der Walle, & Waigh, 2008). Current elastic deformation experimental models are unable to distinguish between the resistant and non-resistant strains bacterial cell surface and substrate enveloped by systematic interventions. Therefore, we utilized AFM methods to estimate deformation and elastic deformation of adhering bacteria in our AgNP resistant bacteria to determine if acquisition of this trait might potentially contribute to their potential biofilm formation.

3.3.3 AFM Image Bacterial Preparation

Glass slides (Gerhard Menzel GmbH, Braunschweig, Germany) were sonicated for 5 min in acetone, ethanol, and DI water and dried with Nitrogen gas and then plasma cleaned for 3 min using PC-2000 Plasma cleaner (South Bay technology, San Clemente, CA). The glass slides were coated with 0.01% poly-D-lysine with a molecular weight of 70,000 to 150,000 and allowed to dry for 10 minutes (Chen et al., 2014).Deflection sensitivity and force constant were calculated and applied for the measurements using thermal calibration. The speed rate for the peizo was between 5 μm/S. The range was between 1-3 μm and the measurement period was one second. Each of the cells was measured 50 times. The surface deflection and adhesion forces were also measured and

calculated for all applied interventions. We used AFM Agilent model 5600LS. The force spectroscopy analysis was performed using R software RX64 3.0.2.The results are shown in figure 10.

3.4 Growth Assays

The ability of the bacteria to grow in response to silver was determined by exposing them to varying concentrations of spherical silver nanoparticles of 10 nm and 40 nm diameter sizes, and of different coating, citrate and PVP (obtained from NanoComposix, San diego, CA) and bulk silver nitrate (Fisher Scientific, Fair Lawn, NJ). We determined that the different-sized silver nanoparticles and bulk silver nitrate were effective over different concentration ranges replicating the findings of earlier researchers (e.g. Morones et al. 2005;(J. R. Morones et al., 2005) . Therefore we assayed the effectiveness of 10 nm particles at concentrations of 100 µg/l, 250 µg/l, 500 µg/l, 750 µg/l, and 1000 µg/l. 40 nm particles were evaluated at 2000 µg/l, 4000 µg/l, 5000 µg/l, and 6000 µg/l. Bulk silver nitrate was evaluated at 50 µg/l, 100 µg/l, 250 µg/l, 500 µg/l, 1000 µg/l, and 2000 µg/l.

The control ($C_1 – C_5$) and treatment ($T_1 – T_5$) populations were cultured for a total of 305 generations**.** Replicates were propagated by daily transfers of 0.1 ml of each culture into 9.9 ml of DMB, allowing populations sizes to fluctuate daily between 5 $*10^6$ cells per ml at the transfer bottleneck to 5 $*10^8$ cells per ml, for a total of ~6.64 generations of binary fission by 2 $\log^{10}$ increase of the cells/ml (Lenski et al. 1991).

All silver treatments were compared to equivalent inoculates of bacteria growing in DMB medium without silver (control). Population growth in response to silver was

measured by optical density and by determining colony forming units (CFU) via serial transfer on DMB agar plates at 0 and 24 hours. Two plates were prepared for each treatment in each experiment. The optical density was determined as an estimate of the cell density of bacteria at 620 nm absorbance using a multi-mode single-channel monochromator-based microplate reader. Optical density readings were taken at 0, 3, 6, 12, and 24 hours of growth. Optical density readings were recorded twice for each treatment in each experiment.

Population samples of all 10 samples took at regular intervals between the sequential transfers. The optical density was accounted for the cell density measurement of bacteria at 620 nm absorbance using multi-mode single-channel monochromator based microplate reader. Colony forming Units (CFU) experiment using Davis minimum Agar plates were conducted for our 0 and hour 24 of each treatment (Bennett, Dao, & Lenski, 1990) consecutive days. Once this had occurred, each control replicate ($C_1 \ldots C_5$) was divided in two, one portion will be designated as $T_1 \ldots T_5$. A sample was kept in -80 freezer for further analysis by following protocol:

- 10 large and 10 small freezer vials were labelled.
- 1 ml glycerol was added to each flask and mixed well
- 1 ml to 1.5 ml centrifuge tubes and 5 ml to 15 ml centrifuge tubes were added and kept in appropriate freezer box

Mean fitness of the stocks growing in different concentrations of silver (AgNPs and AgNO3) was measured at several generations. This was accomplished by

measuring the survival and colony growth of treatment and control stocks in the presence of AgNPs and without them (ancestral environment.).

3.5 Phenotyping Results

Figure 1 shows population growth as measured by the mean optical density of the bacteria at generation 250 in the presence of 40 nm citrate-coated silver nanoparticles at varying concentrations for the treatment and control bacteria. The bacteria assayed in these figures represent a cocktail generated from mixing equal volumes of all five replicate lines of control and treatment ($C_1 - C_5$ and $T_1 - T_5$). The mean standard deviation of all optical density measurements was 0.005. Given these small values, none of the standard deviations are shown in there optical density figures. Figure 1 shows that there is no apparent growth of the bacteria at any of the concentrations assayed (2000, 4000, 5000, and 6000 μg/l) for control bacteria. In the treatment bacteria, there is significant growth for 2000 and 4000 μg/l as well as5000 μg/l especially at stationary phase. In figure 2, population growth of control and treatment bacteria exposed to 40 nm PVP coated silver nanoparticle is shown. In this figure, the treatment bacteria are shown to grow at hour 6 at all concentrations compare to controls. The controls show slow growth after hour 12 and at hour 24. Figure 3 and 4 shows again that the treatment populations have higher growth in 10 nm citrate and PVP coated silver nanoparticles respectively relative to controls. In these figures, 1000 μg/l concentration of 10 nm citrate and PVP coated nanoparticles prevents growth in both strains. This demonstrates stronger antimicrobial effect of smaller size nanoparticles without coating effect considerations.

Figure 3 shows that citrate coated 10 nm AgNPs at eliminated growth in the control strain at concentrations > 250 µg/l; however the treatment populations were able to grow effectively (after a 6 hour lag) at concentrations up to and including 750 µg/l. At 1000 mg/l growth was completely eliminated in the control, yet some modest growth was observed in the treatment population. Figure 4 demonstrated that 10nm PVP-coated AgNPs eliminate growth in the controls at concentrations > 250 µg/l. There is an indication of some growth in the control population at 750 µg/l and no growth in the treatment at this concentration. However, this result is entirely inconsistent with all other measurements, and could have resulted from an error in labeling. Figure 5 shows the effect of bulk silver nitrate against the control and treatment populations by optical density measurements. At concentrations of 500 µg/l and greater there is no observed growth of control bacteria. In the treatment population, growth is observed at concentrations > 250 – 1000 µg/l. No growth is observed at 2000 µg/l. Figures 6a-e are showing colony forming unit (CFU) log 10 differences between hour 0 and hour 24 of the two strains across concentrations using nonlinear log regression. More than 5 log reduction was observed using 10 nm citrate coated silver nanoparticles on control bacteria and this reduction was less than 3 log 10 CFU for 10 nm PVP coated. In treatment bacteria 10 nm citrate and PVP coated nanoparticles results were somewhat similar to each other. There was a less than 3 log 10 CFU on both PVP and citrate coated 10 nm particles. Due to the fact that 40nm AgNPs are much less effective than the 10nm size, a much higher concentration is required to achieve anti-microbial effects (Tajkarimi et al. 2014.) In 40 nm citrate coated bacteria, control bacteria showed significant higher

(more than 3 log 10 CFU) antimicrobial effect at 6000 □g/L concentration compared to the same size PVP coated particles. In treatment population bacteria there was not a significant difference between citrate and PVP coated bacteria at all concentrations assayed. Bulk silver nitrate showed more than 5 log reductions at 1000 µg/l concentration and about 3 $\log^{10}$ reduction for the treatment populations. Table 3 compares the relative effectiveness of bulk silver, 10nm citrate-coated, and 10nm PVP-coated bacteria by CFU reduction from 100 – 500 µg/L. The average reduction for 10nm citrate-coated AgNPs > bulk silver > 10nm PVP-coated over this concentration range for both controls and treatment populations.

Table 4 shows the minimum inhibitory concentrations (MIC) as determined by the microdilution test at generation 300 for the control and treatment replicates (C_1—C_5 and T_1—T_5). The MICs were determined for five forms of silver; 10nm citrate-coated AgNPs, 10nm PVP-coated AgNPs, 40nm citrate-coated AgNPs, 40 nm PVP-coated AgNPs and bBulk silver nitrate ($AgNO_3$). Due to the way the MICs are determined, some of the values read as a range (e.g. 10 – 25 mg/L) or as an inequality (> 25 mg/L). For statistical analysis, is a range was determined, the mean value was used in the calculation. If an inequality was determined, than a minimal integer value greater than the inequality was used (so > 25, became 26 in the calculation.) The latter method is statistically conservative. For the 10nm citrate-coated and 10nm PVP-coated AgNP MIC's the mean MIC of the treatment populations were statistically significantly different from the controls as tested by nested ANOVA; $F = 66.61$, $p < 0.0001$; and $F = 8.65$, $p < 0.019$ respectively. In the case of the 40nm citrate-coated AgNP MICs the mean MIC of the

treatment populations were statistically significantly different from the controls; $F = 101.44$, $p < 0.0001$. No test was performed to determine the MIC of 40nm PVP-coated AgNPs (none were available.) Finally, for bulk silver the mean MIC of the treatment populations were also statistically significantly different from the controls; $F = 101.44$, $p < 0.0001$. The values in table 4 show that the ratios of difference for the silver forms by treatment compared to control populations were 10nm citrate-coated (4.66); 10nm PVP-coated (1.44); 40nm citrate-coated (1.70); and bulk silver (26.2)!

Figure 7a and b show Scanning Electron Microscope (SEM) images of treated and non-treated bacteria with 40 nm PVP-coated silver nanoparticles. Figure 7b illustrates coagulations of silver nanoparticles on the surface of bacteria compared to non-treated bacteria. Figure 8a and b compare the AFM image of control bacteria in the presence of bacterial with AgNPs. This image was taken using the tapping mode (Terri A. Camesano, 1995). Both of these images illustrate association of silver nanoparticles with the bacterial cell wall compared to the control treatment without silver nanoparticles. The AFM image of the treated cell shows apparent damage to the cell wall compared to the untreated control.

Figure 9 shows the disc diffusion assay results comparing standardized control treatment population *E. coli* exposed to different concentrations of 10 nm citrate coated AgNPs as well as 30 μg chloramphenicol disks as a positive control. The control populations are equally inhibited by both concentrations of AgNPs in the solid medium. However, the treatment populations show a smaller zone of inhibition compared to

control populations at both concentrations. In addition the inhibition zone for the treatment populations is smaller at the lower concentration. In addition the zone of inhibition caused by the chloramphenicol seems to be larger in the treatment population disk.

CHAPTER IV

GENOMICS OF SILVER NANOPARTICLE RESISTANCE

Whole genome resequencing was utilized to identify genomic variants associated with the greater AgNP and bulk silver resistance of the treatment populations compared to the controls. This technique has been used by other researchers to identify genomic variants generated from laboratory experimental evolution in *E. coli* (e.g. Herring et al. 2006; Barrick and Lenski 2009). DNA was extracted from each replicate population (generation 100, generation 150, generation 200) that had been stored in the -80ºC freezer ($C_1 - C_5$; $T_1 - T_5$) as well as from the ancestral population *E. coli* K12 MG1655 obtained from ATCC (designated C_0) for the genomic studies. The sample of cells used for extraction came after each population was allowed to grow for 24 hours in standard DM broth (without AgNPs). Cell density was approximately 10^8 cells/ml. Extraction of DNA followed the protocol from Nucleic Acid Sample Preparation for Downstream Analysis: Principles & Methods (GE Health Life Sciences, 2014: http://www.gelifesciences.com/webapp/wcs/stores/servlet/catalog/en/GELifeSciences-US/applications/nucleic-acid-sample-preparation/). DNA from generation 150 (C_1—C_5; T_1—T_5) as well as the ancestral population (C_0) was sent to the Michigan State University core sequencing facility. There genomic libraries were prepared for Illumina sequencing, and these were sequenced on an Illumina HiSeq 2000 platform. In the first run, average read coverage was between 16.2 – 42.7X. For this reason, G150 DNA was

sequenced again to improve the coverage to between 40 – 60 X for all reads. The data reported in this study for G150 are from the 2nd run.

The generation 100 and 200 samples were sequenced at the JSNN on our Illumina MiSeq sequencing platform. The quantity of the extracted DNA (at least 3 ng per sample) was assessed using our Promega Quantus™ Fluorometer. This quantity is required to use the Illumina Nextra XT kit for preparing the genomic library for sequencing. The Illumina Nextera XT kit prepares fragments of DNA that range from about 250—1,500 base pairs (bps) long. The fragments are then ligated to adapters that both connect the DNA to the MiSeq flow cell and include a DNA sequence that "barcodes" the sample for later identification. Finally before sequencing the genomic library fragment lengths must be quantified. This was accomplished by use of the Agilent Bioanalyzer. The bioanalyzer demonstrated that our genomic libraries fit the requirements for an effective run of the MiSeq sequencing platform. The genome size of *E, coli* K12 MG1655 is listed at 4,641,653 bps and is a circular single-stranded DNA chromosome (http://www.ncbi.nlm.nih.gov/nuccore/U00096.3) The MiSeq sequencing platform sequenced both the generation 100 and 200 samples in about 24 hours each. The sequence reads were deposited in our Illumina Basespace@ account in both .fastq and .bam formats.

Prior to sequence alignment and variant calling, the Illumina adapter sequences must be removed from the MiSeq reads. This was accomplished via the use of Partek. Partek is an enterprise level bioinformatics tool. North Carolina A&T State University

version of this program is maintained by Dr. Scott H. Harrison of the Biology department. Sequence alignment and variant calling from the generation 100 and 200 samples was achieved by use of the breseq 0.24rc6 pipeline developed by the Barrick Laboratory at the University of Texas (http://barricklab.org/twiki/bin/view/Lab/ToolsBacterialGenomeResequencing). This pipeline has been used in a number of genomic studies of bacteria (Barrick and Lenski 2009; Deatherage and Barrick 2014). The ***breseq*** program is a computational pipeline for finding mutations relative to a reference sequence in short-read DNA re-sequencing data for microbial sized genomes. The ***breseq*** program is a command line tool implemented in C++ and R. The pipeline accomplishes alignment to the reference genome via the Bowtie 2 algorithm and calls variants via the Sequence Alignment Map (SAMtools) algorithm. Both Mr. Tajkarimi and Dr. Graves received training on the use of this pipeline directly from Dr. Jeffrey Barrick (a collaborator through the Biocomputational Evolution in Action, BEACON National Science Foundation Science Technology Center.) The breseq program is capable of identifying genomic variants including single nucleotide polymorphisms (SNPs), indel (insertion-deletion polymorphisms), and insertion elements (IS, transposons).

Table 5a, b show the genomic variants that exist in the ATCC@ strain of *E. coli* K12 MG1655 compared to the reference genome. There are 3 point mutations, 3 deletions (one large 776 bps), and 2 insertions. The 776 bp deletion in the crl gene at position 257,908 was found in all reads, and thus can be inferred to be fixed in this strain

of MG1655. Also fixed are the deletions in the gatC pseudogene, and the insertions at the intergenic positions 3,560,455 and 4,296,380. Table 6a, b shows the genetic variants compared to the reference genome in the control populations (C_1—C_5) at generation 100. These variants were called in **breseq's** consensus mode. Consensus mode only calls variants that are fixed in the reads (seen in all reads at that position.) The polymorphism mode calls many more variants; the vast majority of these are at very low frequency (~0.001 – 0.01). Mutations at very low frequency are most likely the result of genetic drift and not natural selection therefore are not of interest in attempting to reveal the genomic basis of adaptation to any specific environment. Four of the ancestral mutations were called (deletions in crl, and gatC; insertions in the intergenics). However, new mutations are also called at generation 100 in the control populations. Three of these mutations are found in three or more populations and thus likely represent adaptations (1,999 bp deletion between ychE and oppA; 776 bp deletion in insB-insA; and 4 bp insertion in insA-uspC.) There are an additional three mutations that are unique to specific replicate (most likely representing genetic drift, insertion element adding 9 bps to ybhl; insertion element adding 4 bps to menC; and a point mutation in rpoA.) Table 7a, b shows the genomic variants called in the treatment populations (selected for AgNP resistance) in generation 100. The treatment populations retained four of the ancestral mutations (same as controls). In addition, there were three mutations that were identical to the control populations (oppA, insB1-insA, insA—uspC; thus most likely related to shared features of the culture regime). However the remaining mutations were unique to

the treatment populations (point mutation in cusS, at position 593497; point mutation intergenic at position 3,815,808 between pyrE and rph; and a point mutation in rpoB at position 4,182,803). The latter mutation was shared by four of the five replicates. Table 8a, b shows the genomic variants called in both the control and treatment populations in generation 150. Generation 150 reads were generated from the Michigan State University sequencing center on the Illumina HiSeq 200. However the reads showed high consistency with those generated on the JSNN's MiSeq system. The generation 150 data showed 13 mutations that were probably ancestral (shared by both controls and treatment populations, many of these matched the ancestral mutations that had been identified from the generation 100 sequencing.) Two of the mutations were control adaptations shared by the control populations; seven mutations were unique to specific control populations. Ten unique mutations were identified in the treatment populations. Of these mutations, 8 were found in the T_3 replicate, 1 in T_1, and 1 in T_5. Of the mutations in the T3 replicate, the mutations in cusS, purL, rpoB, and ompR are most interesting (as subsequent analysis of generation 200 variants revealed.) Table 9a, b show the genomic variants called in both control and treatment populations for generation 200. Four of the ancestral mutations are scored for both control and treatment populations, three mutations are shown that are shared by both control and treatment populations (these were scored in previous generations), one shared mutation in the controls (RNA polymerase C, position 4,186,532), and two unique to control replicates (ccmE, position 2,295,168 and rpoA, position 3,440,459.) The silver resistant mutations

shared by all replicate treatment populations were cusS, position 593,467 first scored in replicate T_4 in generation 100 and rpoB, position 4,182,820, first called in replicate T_3 in generation 150. In addition, the mutation in purL at 2,694,130 is shared by 4 of the five treatment replicates. This mutation was also first called in replicate T_3 in generation 150. There are also 3 unique indel mutations in T_1, T_2, T_5 in ompR (positions 3,536,265; 3,536,342; and 3,536,570.)

CHAPTER V

DISCUSSION AND SIGNIFICANCE

Engineered metallic and metallic oxide nanomaterials are being used in an increasing number of applications. Models suggested that the concentration of silver nanoparticles found in European surface waters in 2009 was 0.088 mg/L/year (Gottschalk et al. 2009.) Historical evidence that agriculture and aquaculture are fertile grounds driving the evolution of both heavy metal and antibiotic resistance (Seiler and Berendonk 2012.) Previous research concerning heavy metal resistance in bacteria has not focused on resistance to nano-metals (Silver and Phung 2005; Mijnendonckx et al. 2013.) So far there is only one report in the literature describing the isolation of nanosilver resistant bacterium. This study (Gunawan et al. 2013) accidentally isolated a resistant bacterium in a culture of *E. coli* that became contaminated with a *Bacillus* sp. of unknown origin. They reported that the *Bacillus sp*. was nanosilver resistant. This study specifically evolved resistance to 10nm citrate-coated nanoparticles and tested the resistant bacteria against a variety of nanoparticles and bulk silver nitrate.

This project was motivated by the fact that antimicrobial resistance is a growing worldwide public health issue for humans. Drug and antiseptic resistant (MDR) bacteria are contaminating food and causing dangerously untreatable clinical infections. This

situation requires novel treatment strategies to control MDR pathogenic microorganisms (Chait et al., 2012; Durso et al., 2012; Mellata, 2013) As silver nanoparticles are being proposed as the new antidote for such bacteria (e.g. Lara et al. 2011; Rai et al. 2012) it is a crucial to determine how quickly and effectively bacteria can evolve resistance to them. To address this possibility this study utilized laboratory experimental evolution with *Escherichia coli* as a model system (Tyerman et al., 2013). Experimental evolution has been used to show genomic changes in E. coli both on short long term time scales (Lenski and Travisano 1994; Herring 2006.)

Silver and Phung (2005) showed that such heavy metal transporting mechanisms are widespread in bacteria. *E. coli* K12 MG1655 was chosen because it genome has been fully sequenced and does not normally carry silver resistance genetic elements (sil.) Bacteria with such elements can show 100-fold greater MICs than those without (Silver and Phung 2005; Mijnendonckx 2013). However, *E. coli* K12 MG1655 does not some genetic elements that have been associated with heavy metal resistance. For example, copA (position 510,603—508,099), that codes for the p-type ATP-ase which inducible in the presence of either copper or silver, catalyzes the efflux of both metals. Also, cusS has been shown to be involved in effluxing both copper and silver (Munson et al. 2000; Franke, Grass, and Nies 2001; Gudipathy and McEvoy 2014).

Li et al. 1997 was an earlier experiment that isolated silver resistant *E. coli* mutants on solid media. This experiment utilized bulk silver nitrate ($AgNO_3$) and silver sulfadiazine (AgSD.) They were able to increase the silver resistance of the mutant strains by 128 times for ($AgNO_3$) and 64 times for (AgSD). They also noted that their

silver resistant mutants had reduced susceptibility to cephalosporins (4 fold decrease in MICs); and possibly tetracycline and chloramphenicol. This result suggests that their mutants were pleiotropic (affecting more than one trait simultaneously.) This study was conducted before the wide spread availability of whole genome sequencing, but they were able to use protein-gel electrophoresis to show that their mutant strains were deficient in the activity of the proteins OmpF, OmpC, and OmpA. These proteins are called "porins" and they influence the permeability of the bacterial outer membrane. Li et al. 1997 concluded that the resistance of these mutants to Ag+ and antibiotics was due to decreased permeability of the outer membrane to these substances.

This study showed that by generation 250 the treatment bacteria had greater AgNP as well as bulk silver ($AgNO_3$) resistance at a range of concentrations compared to the controls. The minimum inhibitory concentrations at generation 300 showed that treatment replicates had greater silver resistance for all types of silver measured (Table 4a,b). In addition by generation 305 that the treatment populations had increased their bulk $AgNO_3$ resistance by ~ 100x at 100 µg/l relative to the controls and ~10X at 250 µg/L relative to the controls (Figures 6a--e.) The resistance to AgNPs depended on size and coating. However, the treatment populations performed better than the controls across the range of concentrations studied (Table 3, Figures 6a—e). These results indicate that the selection protocol produced bacteria that were resistant to both AgNPs and bulk silver. It is still unclear whether these resistances differ. Some studies suggest that the mechanism of action for metallic nanoparticles are only due to the release of the metal ion (Xiu et al. 2012); while others suggest that the particle itself may play a role

independent from the coating type (Bandyopathy et al. 2012). Our laboratory is currently engaged in research that will further separate metal ion from nano-size effects.

The genomic analysis allows us to observe the increase in silver resistance mutants from the ancestral population (C_0), through treatment populations from generations 100, 150, and 200. Unfortunately time and funding did not allow us to sequence generation 250 or 300. Therefore it is possible and even likely that additional silver resistance mutations had accumulated in the treatment populations in the period between the sequencing and the last phenotyping (G300). However the genomic analysis makes clear that the treatment populations had accumulated three major mutations by generation 200 that partially accounts for their greater silver resistance (cusS, 593,467, T—G, D435A or aspartate (electrically charged -) to alanine (hydrophobic) at position 435; purL, 2,694,130, G—T, R191C or Arginine (electrically charged +) to Cysteine (hydrophilic); and rpoB, 4,182,820, C—T, H526Y or histidine (electrically charged +) to tyrosine (hydrophilic). The cusS mutation occurs within the histidine-kinase, DNA gyrase B, and HSP90-like ATPase site of the protein (ecogene; http://www.kegg.jp/ssdb-bin/ssdb_motif?kid=eco:b0570). The purL mutation occurs within prior to the enzyme's active sites (257—389; 432—589; and 822—966; ecogene, http://www.kegg.jp/ssdb-bin/ssdb_motif?kid=eco:b2557). The rpoB mutation occurs within the Rpb2 domain 3 site of the RNA polymerase B (ecogene; http://www.kegg.jp/ssdb-bin/ssdb_motif?kid=eco:b3987). Thus all of these mutations are non-synonymous and two of them occur within an active site of a protein.

The identification of a mutation in cusS that contributes to AgNP resistance in the treatment lines is not surprising. This is supported by its known function and previous experiments (Lok et al. 2008; Gudipathy and McEvoy 2014). However, this specific mutation has not been reported before. The purL (phosphoribosylformyl-glycineamide synthetase) gene plays a role in purine synthesis (Sampei and Mizobuchi 1989). Its mechanistic relationship to silver resistance is not immediately clear. Mutations in the rpoB (RNA polymerase B) gene have been linked with antibiotic resistance (Romero and Casedsús 2014) as well as increased evolvability (Barrick et al 2013.) Both of these traits could conceivably contribute to silver AgNP or $AgNO_3$ resistance. This result specifically predicts that these mutations may be pleiotropic, thus it is likely that the AgNP resistant bacteria could be resistant to other environmental insults, including antibiotic resistance. Subsequent experiments will be required to test these possibilities.

In conclusion, this study has shown that bacteria are capable of rapidly evolving de novo resistance to AgNPs (~250 generations or about 38 days.) This experiment cannot determine if the resistance resulted from a "hard" or "soft" sweep of mutations. A hard sweep results from de-novo mutations starting at very low frequency and then sweeping to fixation in a specific environment. Soft sweeps begin with existing genetic variants that are maintained in the population at very low frequency. While none of the high frequency mutations scored in the treatment populations (T_1—T_5) at generation 200 were found in the ancestral lines (C_0); this does not mean that they were not there at frequencies undetectable by our sequencing. In addition, there is evidence that the process of cocktailing the treatment populations in generation 140 may have led to a

"sweep" by the T_3 replicate in the treatment populations. T_3 was the only population that had all three of the cusS, purl, and rpoB mutations. Finally, given that we did not sequence generation 250 and 300, we do not know if additional mutations at low frequency did not sweep to consensus. This will be tested in subsequent studies. In addition, Figure 8 shows via atomic force microscopy (AFM) that there seems to be clear physical differences in the cell wall characteristics of the control and treatment lines by generation 250. It seems unlikely that such strong phenotypic differences are caused by only three point mutations. This suggests that in addition to the genomic differences we measured between the control and treatment populations that there may be transcriptomic differences as well. For example, Lok et al. 2010 utilizing the silver resistant mutants first scored by Li, Hiroshi, and Williams (1997) showed significant gene expression pattern differences in the mutant strains compared to controls by two-dimensional gel electrophoresis and mass spectrometry. Future studies in the experimental evolution of silver nanoparticle resistance will need to utilize RNAseq methods in addition to genomic resequencing to more fully understand the mechanisms of resistance.

The rapid evolution of silver nanoparticle resistance in an "off the shelf" laboratory bacterium does not bode well for the sustainability of silver nanoparticles in antimicrobial applications. Table 1 shows that *E. coli* K12 MG1655 had few resistance elements of any kind. Yet we know that silver resistant bacteria already exist in nature (Mijnendonckx 2013; Graves 2014). Zhang, Liang, and Hu 2013 have shown the increase in expression of the silE gene in bacterial communities isolated from sludge water in a bioreactor system. Silver resistance as well as antibiotic resistance is carried

on plasmids. This means that they can be horizontally transmitted between widely separated groups of bacteria. Indeed, nanoalumina has been demonstrated to increase the rate of plasmid transfer (Qiu 2012). It is not known whether other nanometals would have this effect.

This means that there is a crucial need for more studies of the impact of metallic or metallic oxide nanoparticles on a wider variety of bacteria and bacterial communities. For example, given that the mechanisms of antibiotic and metal resistance are often shared, it might not take MDR bacteria long to evolve resistance of metallic nanoparticles. Should this occur, the use of metallic nanoparticles would enter a cycle of increasing concentration to effect desired result (a treadmill, similar to that observed in pesticide and antibiotic use.) Given that the attractiveness of metallic and metallic oxide nanoparticles results from their current effectiveness against bacteria at low concentration along with their low toxicity against mammalian cells in their effective range, increasing resistance would eliminate their usefulness.

REFERENCES

Baker, C., Pradhan, A., Pakstis, L., Pochan, D. J., & Shah, S. I. (2005). Synthesis and antibacterial properties of silver nanoparticles. *J Nanosci Nanotechnol, 5*(2), 244-249.

Bauer, A. W., Kirby, W. M. M., Sherris, J. C., & Turck, M. (1966). Antibiotic Susceptibility Testing by a Standardized Single Disk Method. *American Journal of Clinical Pathology, 45*(4), 493-&.

Bednorz, C., Oelgeschlager, K., Kinnemann, B., Hartmann, S., Neumann, K., Pieper, R., . . . Guenther, S. (2013). The broader context of antibiotic resistance: Zinc feed supplementation of piglets increases the proportion of multi-resistant Escherichia coli in vivo. *International Journal of Medical Microbiology, 303*(6-7), 396-403. doi: 10.1016/j.ijmm.2013.06.004

Bennett, A. F., Dao, K. M., & Lenski, R. E. (1990). Rapid evolution in response to high-temperature selection. *Nature, 346*(6279), 79-81. doi: 10.1038/346079a0

Bharitkar, Y. P., Bathini, S., Ojha, D., Ghosh, S., Mukherjee, H., Kuotsu, K., . . . Mondal, N. B. (2014). Antibacterial and antiviral evaluation of sulfonoquinovosyldiacylglyceride: a glycolipid isolated from Azadirachta indica leaves. *Letters in Applied Microbiology, 58*(2), 184-189. doi: 10.1111/lam.12174

Birla, S. S., Tiwari, V. V., Gade, A. K., Ingle, A. P., Yadav, A. P., & Rai, M. K. (2009). Fabrication of silver nanoparticles by Phoma glomerata and its combined effect against Escherichia coli, Pseudomonas aeruginosa and Staphylococcus aureus. *Letters in Applied Microbiology, 48*(2), 173-179. doi: 10.1111/j.1472-765X.2008.02510.x

Bonhoeffer, S., Lipsitch, M., & Levin, B. R. (1997). Evaluating treatment protocols to prevent antibiotic resistance. *Proc Natl Acad Sci U S A, 94*(22), 12106-12111.

Bradford, A., Handy, R. D., Readman, J. W., Atfield, A., & Muhling, M. (2009). Impact of silver nanoparticle contamination on the genetic diversity of natural bacterial assemblages in estuarine sediments. *Environmental Science & Technology, 43*(12), 4530-4536.

Burchardt, A. D., Carvalho, R. N., Valente, A., Nativo, P., Gilliland, D., Garcia, C. P., . . . Lettieri, T. (2012). Effects of silver nanoparticles in diatom Thalassiosira pseudonana and cyanobacterium Synechococcus sp. *Environmental Science & Technology, 46*(20), 11336-11344. doi: 10.1021/es300989e

Castellano, J. J., Shafii, S. M., Ko, F., Donate, G., Wright, T. E., Mannari, R. J., . . . Robson, M. C. (2007). Comparative evaluation of silver-containing antimicrobial dressings and drugs. *Int Wound J, 4*(2), 114-122. doi: 10.1111/j.1742-481X.2007.00316.x

CDC. (2012). About Antimicrobial Resistance: A Brief Overview: CDC.

Chait, R., Vetsigian, K., & Kishony, R. (2012). What counters antibiotic resistance in nature? *Nature Chemical Biology, 8*(1), 2-5. doi: 10.1038/nchembio.745

Chen, Y., Harapanahalli, A. K., Busscher, H. J., Norde, W., & van der Mei, H. C. (2014). Nanoscale cell wall deformation impacts long-range bacterial adhesion forces on surfaces. *Appl Environ Microbiol, 80*(2), 637-643. doi: 10.1128/AEM.02745-13

Childers, B. M., Van Laar, T. A., You, T., Clegg, S., & Leung, K. P. (2013). MrkD(1P) from Klebsiella pneumoniae Strain IA565 Allows for Coexistence with Pseudomonas aeruginosa and Protection from Protease-Mediated Biofilm Detachment. *Infection and Immunity, 81*(11), 4112-4120. doi: Doi 10.1128/Iai.00521-13

Dobias, J., & Bernier-Latmani, R. (2013). Silver release from silver nanoparticles in natural waters. *Environmental Science & Technology, 47*(9), 4140-4146. doi: 10.1021/es304023p

Dufrene, Y. F., & Pelling, A. E. (2013). Force nanoscopy of cell mechanics and cell adhesion. *Nanoscale, 5*(10), 4094-4104. doi: 10.1039/c3nr00340j

Durso, L. M., Miller, D. N., & Wienhold, B. J. (2012). Distribution and quantification of antibiotic resistant genes and bacteria across agricultural and non-agricultural metagenomes. *PLoS One, 7*(11), e48325. doi: 10.1371/journal.pone.0048325

El Badawy, A. M., Silva, R. G., Morris, B., Scheckel, K. G., Suidan, M. T., & Tolaymat, T. M. (2011). Surface charge-dependent toxicity of silver nanoparticles. *Environmental Science & Technology, 45*(1), 283-287. doi: 10.1021/es1034188

Furuya, E. Y., & Lowy, F. D. (2006). Antimicrobial-resistant bacteria in the community setting. *Nature Reviews Microbiology, 4*(1), 36-45. doi: Doi 10.1038/Nrmicro1325

Gomez-Sanz, E., Kadlec, K., Fessler, A. T., Zarazaga, M., Torres, C., & Schwarz, S. (2013). Novel erm(T)-Carrying Multiresistance Plasmids from Porcine and Human Isolates of Methicillin-Resistant Staphylococcus aureus ST398 That Also Harbor Cadmium and Copper Resistance Determinants. *Antimicrobial Agents and Chemotherapy, 57*(7), 3275-3282. doi: Doi 10.1128/Aac.00171-13

Gupta, A., & Silver, S. (1998). Molecular Genetics: Silver as a biocide: Will resistance become a problem? *Nat Biotech, 16*(10), 888-888.

Hacioglu, N., & Tosunoglu, M. (2014). Determination of antimicrobial and heavy metal resistance profiles of some bacteria isolated from aquatic amphibian and reptile species. *Environmental Monitoring and Assessment, 186*(1), 407-413. doi: DOI 10.1007/s10661-013-3385-y

Hajmeer, M. N., Tajkarimi, M., Gomez, E. L., Lim, N., O'Hara, M., Riemann, H. P., & Cliver, D. O. (2011). Thermal death of bacterial pathogens in linguica smoking. *Food Control, 22*(5), 668-672. doi: DOI 10.1016/j.foodcont.2010.07.027

Haraguchi, A., Miura, M., Fujise, O., Hamachi, T., & Nishimura, F. (2014). Porphyromonas gingivalis gingipain is involved in the detachment and aggregation of Aggregatibacter actinomycetemcomitans biofilm. *Molecular Oral Microbiology, 29*(3), 131-143. doi: Doi 10.1111/Omi.12051

Holzel, C. S., Muller, C., Harms, K. S., Mikolajewski, S., Schafer, S., Schwaiger, K., & Bauer, J. (2012). Heavy metals in liquid pig manure in light of bacterial antimicrobial resistance. *Environmental Research, 113*, 21-27. doi: DOI 10.1016/j.envres.2012.01.002

Jain, J., Arora, S., Rajwade, J. M., Omray, P., Khandelwal, S., & Paknikar, K. M. (2009). Silver Nanoparticles in Therapeutics: Development of an Antimicrobial Gel Formulation for Topical Use. *Molecular Pharmaceutics, 6*(5), 1388-1401. doi: Doi 10.1021/Mp900056g

Jones, K. E., Patel, N. G., Levy, M. A., Storeygard, A., Balk, D., Gittleman, J. L., & Daszak, P. (2008). Global trends in emerging infectious diseases. *Nature, 451*(7181), 990-U994. doi: Doi 10.1038/Nature06536

Kedziora, A., Gerasymchuk, Y., Sroka, E., Bugla-Ploskonska, G., Doroszkiewicz, W., Rybak, Z., . . . Strek, W. A. (2013). [Use of the materials based on partially reduced graphene-oxide

with silver nanoparticle as bacteriostatic and bactericidal agent]. *Polim Med, 43*(3), 129-134.

Kim, J. S., Kuk, E., Yu, K. N., Kim, J. H., Park, S. J., Lee, H. J., . . . Cho, M. H. (2007). Antimicrobial effects of silver nanoparticles. *Nanomedicine-Nanotechnology Biology and Medicine, 3*(1), 95-101. doi: DOI 10.1016/j.nano.2006.12.001

Klasen, H. J. (2000). A historical review of the use of silver in the treatment of burns. II. Renewed interest for silver. *Burns, 26*(2), 131-138. doi: http://dx.doi.org/10.1016/S0305-4179(99)00116-3

Lenski, R. E. (1998). Bacterial evolution and the cost of antibiotic resistance. *International Microbiology, 1*(4), 265-270.

Madhavan, R. V., Rosemary, M. J., Nandkumar, M. A., Krishnan, K. V., & Krishnan, L. K. (2011). Silver nanoparticle impregnated poly (varepsilon-caprolactone) scaffolds: optimization of antimicrobial and noncytotoxic concentrations. *Tissue Eng Part A, 17*(3-4), 439-449. doi: 10.1089/ten.TEA.2009.0791

Martinez, J. L., & Baquero, F. (2000). Mutation frequencies and antibiotic resistance. *Antimicrob Agents Chemother, 44*(7), 1771-1777.

Mellata, M. (2013). Human and Avian Extraintestinal Pathogenic Escherichia coli: Infections, Zoonotic Risks, and Antibiotic Resistance Trends. *Foodborne Pathogens and Disease*. doi: 10.1089/fpd.2013.1533

Merrifield, D. L., Shaw, B. J., Harper, G. M., Saoud, I. P., Davies, S. J., Handy, R. D., & Henry, T. B. (2013). Ingestion of metal-nanoparticle contaminated food disrupts endogenous microbiota in zebrafish (Danio rerio). *Environmental Pollution, 174*, 157-163. doi: DOI 10.1016/j.envpol.2012.11.017

Mijnendonckx, K., Leys, N., Mahillon, J., Silver, S., & Van Houdt, R. (2013). Antimicrobial silver: uses, toxicity and potential for resistance. *Biometals, 26*(4), 609-621. doi: 10.1007/s10534-013-9645-z

Morones, J. R., Elechiguerra, J. L., Camacho, A., Holt, K., Kouri, J. B., Ramirez, J. T., & Yacaman, M. J. (2005). The bactericidal effect of silver nanoparticles. *Nanotechnology, 16*(10), 2346-2353.

Morones, J. R., Elechiguerra, J. L., Camacho, A., Holt, K., Kouri, J. B., Ramírez, J. T., & Yacaman, M. J. (2005). The bactericidal effect of silver nanoparticles. *Nanotechnology, 16*(10), 2346.

Nelson DuránI, P. D. M., Roseli De ContiI, Oswaldo L. AlvesI, Fabio T. M. CostaII, Marcelo Brocchi. (2010). Potential use of silver nanoparticles on pathogenic bacteria, their toxicity and possible mechanisms of action. *Journal of the Brazilian Chemical Society, 21*(6).

Nunez, M. E., Martin, M. O., Chan, P. H., Duong, L. K., Sindhurakar, A. R., & Spain, E. M. (2005). Atomic force microscopy of bacterial communities. *Environmental Microbiology, 397*, 256-268. doi: Doi 10.1016/S0076-6879(05)97015-8

Olesja Bondarenko, A. I., Aleksandr Ka¨kinen, Imbi Kurvet, Anne Kahru. (2013). Particle-Cell Contact Enhances Antibacterial Activity of Silver Nanoparticles. *PLoS One, 8*(5), 1-12.

Pal, S., Tak, Y. K., & Song, J. M. (2007). Does the antibacterial activity of silver nanoparticles depend on the shape of the nanoparticle? A study of the gram-negative bacterium Escherichia coli. *Applied and Environmental Microbiology, 73*(6), 1712-1720. doi: Doi 10.1128/Aem.02218-06

Panáček, A., Kvítek, L., Prucek, R., Kolář, M., Večeřová, R., Pizúrová, N., . . . Zbořil, R. (2006). Silver Colloid Nanoparticles: Synthesis, Characterization, and Their Antibacterial Activity. *The Journal of Physical Chemistry B, 110*(33), 16248-16253. doi: 10.1021/jp063826h

Prabhu, S., & Poulose, E. (2012). Silver nanoparticles: mechanism of antimicrobial action, synthesis, medical applications, and toxicity effects. *International Nano Letters, 2*(1), 1-10. doi: 10.1186/2228-5326-2-32

Rai, M., Yadav, A., & Gade, A. (2009). Silver nanoparticles as a new generation of antimicrobials. *Biotechnology Advances, 27*(1), 76-83. doi: DOI 10.1016/j.biotechadv.2008.09.002

Rai, M. K., Deshmukh, S. D., Ingle, A. P., & Gade, A. K. (2012). Silver nanoparticles: the powerful nanoweapon against multidrug-resistant bacteria. *Journal of Applied Microbiology, 112*(5), 841-852.

Rai, R. S., & Subramanian, S. (2009). Role of transmission electron microscopy in the semiconductor industry for process development and failure analysis. *Progress in Crystal Growth and Characterization of Materials, 55*(3-4), 63-97. doi: DOI 10.1016/j.pcrysgrow.2009.09.002

Reinsch, B. C., Levard, C., Li, Z., Ma, R., Wise, A., Gregory, K. B., . . . Lowry, G. V. (2012). Sulfidation of Silver Nanoparticles Decreases Escherichia coli Growth Inhibition. *Environmental Science & Technology, 46*(13), 6992-7000. doi: Doi 10.1021/Es203732x

Rogers, S. S., van der Walle, C., & Waigh, T. A. (2008). Microrheology of Bacterial Biofilms In Vitro: Staphylococcus aureus and Pseudomonas aeruginosa. *Langmuir, 24*(23), 13549-13555. doi: Doi 10.1021/La802442d

Salam A. Ibrahim, T. B., Danfeng Song, Mehrdad Tajkarimi. (2011). Survival and Growth Characteristics of Escherichia coli O157:H7 in Pomegranate-Carrot and Pomegranate-Apple Blend Juices. *Food and Nutrition Sciences, 2*, 844-851. doi: 10.4236

Schacht, V. J., Neumann, L. V., Sandhi, S. K., Chen, L., Henning, T., Klar, P. J., . . . Bunge, M. (2013). Effects of silver nanoparticles on microbial growth dynamics. *Journal of Applied Microbiology, 114*(1), 25-35. doi: 10.1111/jam.12000

Schwab, T. E. A. C. a. K. J. (2012). Are nanoparticles a threat to our drinking water? Johns Hopking University Global water program

Shahverdi, A. R., Fakhimi, A., Shahverdi, H. R., & Minaian, S. (2007). Synthesis and effect of silver nanoparticles on the antibacterial activity of different antibiotics against Staphylococcus aureus and Escherichia coli. *Nanomedicine, 3*(2), 168-171.

Shoeb, E., Badar, U., Akhter, J., Shams, H., Sultana, M., & Ansari, M. A. (2012). Horizontal gene transfer of stress resistance genes through plasmid transport. *World Journal of Microbiology & Biotechnology, 28*(3), 1021-1025. doi: DOI 10.1007/s11274-011-0900-6

Silva, A. A. D. E., de Carvalho, M. A. R., de Souza, S. A. L., Dias, P. M. T., da Silva, R. G., Saramago, C. S. D., . . . Hofer, E. (2012). HEAVY METAL TOLERANCE (Cr, Ag AND Hg) IN BACTERIA ISOLATED FROM SEWAGE. *Brazilian Journal of Microbiology, 43*(4), 1620-1631.

Silver, S. (2003). Bacterial silver resistance: molecular biology and uses and misuses of silver compounds. *Fems Microbiology Reviews, 27*(2-3), 341-353. doi: Doi 10.1016/S0168-6445(03)00047-0

Silver, S., & Phung, L. T. (2005). A bacterial view of the periodic table: genes and proteins for toxic inorganic ions. *Journal of Industrial Microbiology & Biotechnology, 32*(11-12), 587-605. doi: DOI 10.1007/s10295-005-0019-6

Singh, P. K., Shiha, M. J., & Kumar, A. (2014). Antibacterial responses of retinal Muller glia: production of antimicrobial peptides, oxidative burst and phagocytosis. *J Neuroinflammation, 11*, 33. doi: 10.1186/1742-2094-11-33

Sondi, I., & Salopek-Sondi, B. (2004). Silver nanoparticles as antimicrobial agent: a case study on E-coli as a model for Gram-negative bacteria. *Journal of Colloid and Interface Science, 275*(1), 177-182. doi: DOI 10.1016/j.jcis.2004.02.012

Tajkarimi, M., & Ibrahim, S. A. (2011). Antimicrobial activity of ascorbic acid alone or in combination with lactic acid on Escherichia coli O157:H7 in laboratory medium and carrot juice. *Food Control, 22*(6), 801-804. doi: 10.1016/j.foodcont.2010.11.030

Tajkarimi, M., Rlemann, H. P., Haji-Neer, M. N., Gomez, E. L., Razavilar, V., & Cliver, D. O. (2008). Ammonia disinfection of animal feeds - Laboratory study. *International Journal of Food Microbiology, 122*(1-2), 23-28. doi: 10.1016/j.ijfoodmicro.2007.11.040

Tajkarimi, M. M., Ibrahim, S. A., & Cliver, D. O. (2010). Antimicrobial herb and spice compounds in food. *Food Control, 21*(9), 1199-1218. doi: 10.1016/j.foodcont.2010.02.003

Terri A. Camesano, M. J. N., and Bruce E. Logan. (1995). Observation of Changes in Bacterial Cell Morphology Using Tapping Mode Atomic Force Microscopy. *Langmuir, 16*, 4563-4572.

Toprak, E., Veres, A., Michel, J. B., Chait, R., Hartl, D. L., & Kishony, R. (2012). Evolutionary paths to antibiotic resistance under dynamically sustained drug selection. *Nature Genetics, 44*(1), 101-105. doi: 10.1038/ng.1034

Tyerman, J. G., Ponciano, J. M., Joyce, P., Forney, L. J., & Harmon, L. J. (2013). The evolution of antibiotic susceptibility and resistance during the formation of Escherichia coli biofilms in the absence of antibiotics. *Bmc Evolutionary Biology, 13*, 22. doi: 10.1186/1471-2148-13-22

Vadillo-Rodriguez, V., Beveridge, T. J., & Dutcher, J. R. (2008). Surface viscoelasticity of individual gram-negative bacterial cells measured using atomic force microscopy. *Journal of Bacteriology, 190*(12), 4225-4232. doi: 10.1128/JB.00132-08

Varela, A. R., & Manaia, C. M. (2013). Human health implications of clinically relevant bacteria in wastewater habitats. *Environmental Science and Pollution Research, 20*(6), 3550-3569. doi: DOI 10.1007/s11356-013-1594-0

Volle, C. B., Ferguson, M. A., Aidala, K. E., Spain, E. M., & Nunez, M. E. (2008). Spring constants and adhesive properties of native bacterial biofilm cells measured by atomic force microscopy. *Colloids Surf B Biointerfaces, 67*(1), 32-40. doi: 10.1016/j.colsurfb.2008.07.021

Wilkinson, L. J., White, R. J., & Chipman, J. K. (2011). Silver and nanoparticles of silver in wound dressings: a review of efficacy and safety. *Journal of Wound Care, 20*(11), 543-549.

Wu, R.-T., & Hsu, S. L.-C. (2008). Preparation of highly concentrated and stable suspensions of silver nanoparticles by an organic base catalyzed reduction reaction. *Materials Research Bulletin, 43*(5), 1276-1281. doi: http://dx.doi.org/10.1016/j.materresbull.2007.05.020

Xiu, Z. M., Zhang, Q. B., Puppala, H. L., Colvin, V. L., & Alvarez, P. J. J. (2012). Negligible Particle-Specific Antibacterial Activity of Silver Nanoparticles. *Nano Letters, 12*(8), 4271-4275. doi: Doi 10.1021/Nl301934w

Yamanaka, M., Hara, K., & Kudo, J. (2005). Bactericidal actions of a silver ion solution on Escherichia coli, studied by energy-filtering transmission electron microscopy and proteomic analysis. *Appl Environ Microbiol, 71*(11), 7589-7593. doi: 10.1128/AEM.71.11.7589-7593.2005

Zhang, M. X., Zhu, C. F., Zhou, Y. J., Le Kong, X., Hider, R. C., & Zhou, T. (2014). Design, Synthesis, and Antimicrobial Evaluation of Hexadentate Hydroxypyridinones with High Iron(III) Affinity. *Chemical Biology & Drug Design*. doi: 10.1111/cbdd.12358

Zhang, Z., Kong, F., Vardhanabhuti, B., Mustapha, A., & Lin, M. (2012). Detection of engineered silver nanoparticle contamination in pears. *J Agric Food Chem, 60*(43), 10762-10767. doi: 10.1021/jf303423q

Zhong, J., & He, D. N. (2012). Recent Progress in the Application of Atomic Force Microscopy for Supported Lipid Bilayers. *Chemistry-a European Journal, 18*(14), 4148-4155. doi: DOI 10.1002/chem.201102831

APPENDIX A

TABLES AND FIGURES

Table 1. Antimicrobial Genes in *Escherichia coli*

Antimicrobial Agent	**Gene/s**	**MG1655**	**Reference**
Streptomycin	aadA1	no	Momtaz et al. 2012
Gentamicin	aac(3)-IIV	no	
Sulfonamide	sul1, bla SHV, bla, CMY	no	
Beta lactams	kpc, cmy-2, shv, tem	no	Xia et al. 2011
	ctx-m, lap-1, bla-tem	no	
Ampicillin	ere(A)	no	
Erythromycin	cat A1	no	Momtaz et al. 2012
Chloramphenicol	cm1A	no	
Tetracycline	tet(A), tet(B)	no	
Trimethoprim	dfr A1	no	
Quinolones	qnr A	no	
Sulfonamide	sul1, sul2	no	Tadesse et al. 2012
Silver	silE, sil-CFBA	no	Gupta et al. 2001; Silver 2003
	cusS, ompA, ompB, ompF	yes	Li et al. 1997; Gudipathy & McEvoy 2014

Table 2. Directional Selection for AgNP Resistance

Generations	Exposure Concentration
1 – 50	50 µg/l
51 -- 140	100 µg/l
141 – 265*	125 µg/l
266– 305	125 µg/l

*Replicates were mixed at generation 141 to rescue poor performing populations; samples were taken from the cocktail to reestablish five replicates.

Table 3. Relative Effectiveness of Silver by Type (measured by CFU reduction)

		Control		
		Bulk	10-citrate	10-PVP
Conc.				
	100	-1.00	-1.50	0.50
	250	-1.00	-2.25	-0.25
	500	-1.75	-2.20	-0.75
Mean		-1.25	-1.98	-0.17
SD		0.43	0.42	0.63

		Treatment		
		Bulk	10-citrate	10-PVP
Conc.				
	100	1.00	-1.50	1.00
	250	-0.75	-2.00	1.00
	500	-0.75	2.70	0.25
Mean		-0.17	-0.27	0.75
SD		1.01	2.58	0.43

The relative effectiveness of bulk silver, 10nm citrate-coated AgNPs, and 10nm PVP-coated AgNPs are estimated by CFU reduction of control and treatment populations across three concentrations (100 – 500 μg/L.) These data suggest that effectiveness should be ranked 10nm citrate-coated > bulk silver > 10nm PVP-coated.

Table 4a. Minimum Inhibitory Concentration Determined by Micro Dilution Method at Generation 300

10nm Citrate Coated NPs

C1	5 mg/L	T1	>50 mg/L
C2	5 mg/L	T2	7.5 mg/L
C3	5 mg/L	T3	>50 mg/L
C4	5-7.5 mg/L	T4	7.5 mg/L
C5	5 mg/L	T5	7.5 mg/L
Mean	5.25 mg/L		24.5 mg/L
Std. Dev.	0.56		23.27

10nm PVP Coated NPs

C1	10 mg/L	T1	>25 mg/L
C2	10 mg/L	T2	17.5 mg/L
C3	10-25mg/L	T3	>25 mg/L
C4	10-17.5 mg/L	T4	17.5 mg/L
C5	>25 mg/L	T5	>25 mg/L
Mean	15.25 mg/L		22 mg/L
Std. Dev.	6.27		4.10

40nm Citrate Coated NPs

C1	125 mg/L	**T1**	250 mg/L
C2	125 mg/L	**T2**	125 mg/L
C3	87.5 mg/L	**T3**	250 mg/L
C4	125 mg/L	**T4**	125 mg/L
C5	125 mg/L	**T5**	250 mg/L
Mean	117.5 mg/L		200 mg/L
Std. Dev.	16.77		68.46

Bulk Silver Nitrate ($AgNO_3$) NPs

C1	0.625mg/L	**T1**	25 mg/L
C2	0.625mg/L	**T2**	0.625 mg/L
C3	0.625mg/L	**T3**	25 mg/L
C4	0.625mg/L	**T4**	12.5 mg/L
C5	0.625mg/L	**T5**	12.5-25 mg/L
Mean	0.625 mg/L		16.375 mg/L
Std. Dev.	0.00		10.21

Table 4b. Ratio of Treatment to Control Minimum Inhibitory Concentration (MIC) by Type of Silver Generation 300

Type	Ratio (T/C)	F	p
10 nm Citrate-coated	4.66 – 3.04 X	3.328	< 0.106 ns
10 nm PVP-coated	1.65 – 1.44 X	5.608*	< 0.045
40 nm Citrate-coated	1.70 X	6.849*	< 0.031
Bulk $AgNO_3$	26.2 X	11.64**	< 0.009

Table 5a. Genomic Variants in Ancestral ATCC@ *E. coli* K12 MG1655

	Position	Mutation	Freq.
[crl]	257,908	Δ776 bp	1.000
ylcI ←	580,302	C→T	0.222
gatC ←	2,173,361	Δ2 bp	1.000
gshA ←	2,815,694	A→T	0.182
garK ←	3,271,022	Δ3 bp	0.075
glpR ← / ← glpR	3,560,455	i+G	1.000
gltP → / ← yjcO	4,296,060	C→T	0.333
gltP → / ← yjcO	4,296,380	+CG	1.000

Mutation Description: Δ = deletion; i = insertion; ⟹ = point mutation

Table 5b. Genomic Variants in Ancestral ATCC @*E. coli* K12 MG 1655 (Annotation and Description)

Annotation		Description
[crl]		[crl]
ylcI ←	R48R (AGG→AGA)	DUF3950 family protein, DLP12 prophage
gatC ←	pseudogene (1-2/442 nt)	pseudogene, galactitol-specific enzyme IIC component of PTS*
gshA ←	L249H (CTT→CAT)	glutamate-cysteine ligase
garK ←	coding (747-749/1146 nt)	glycerate kinase I
glpR ← / ← glpR	intergenic (-2/+1)	pseudogene, DNA-binding transcriptional repressor*
gltP → / ← yjcO	intergenic (+266/+376)	glutamate/aspartate:proton symporter/Sel1 family TPR-like repeat protein
gltP → / ← yjcO	intergenic (+586/+56)	glutamate/aspartate:proton symporter/Sel1 family TPR-like repeat protein
Annotation		Description
[crl]		[crl]
ylcI ←	R48R (AGG→AGA)	DUF3950 family protein, DLP12 prophage
gatC ←	pseudogene (1-2/442 nt)	pseudogene, galactitol-specific enzyme IIC component of PTS*
gshA ←	L249H (CTT→CAT)	glutamate-cysteine ligase
garK ←	coding (747-749/1146 nt)	glycerate kinase I
glpR ← / ← glpR	intergenic (-2/+1)	pseudogene, DNA-binding transcriptional repressor*
gltP → / ← yjcO	intergenic (+266/+376)	glutamate/aspartate:proton symporter/Sel1 family TPR-like repeat protein
gltP → / ← yjcO	intergenic (+586/+56)	glutamate/aspartate:proton symporter/Sel1 family TPR-like repeat protein

Table 6a. Genomic Variants in *E. coli* K12 MG1655 (Control Populations) Generation 100

Populations	Gene	Position	Mutation
C_0, C_1, C_2, C_3, C_4, C_5	[crl]	257,908	Δ776 bp
C_1, C_2	ybhI →	802,819	IS1 (+) +9 bp
C_2, C_3, C_4	ychE → / → oppA	1,299,499	Δ1,199 bp
C_1, C_2, C_3, C_5	insB1–insA	1,978,503	Δ776 bp
C_1, C_2, C_3, C_4, C_5	insA ← / → uspC	1,979,486	IS5 (+) +4 bp
C_0, C_1, C_2, C_4, C_5	gatC ←	2,173,361	Δ2 bp
C_4	menC ←	2,375,828	IS186 (+) +4 bp
C_1	rpoA ←	3,440,459	G→A
C_0, C_1, C_2, C_3, C_4, C_5	glpR ← / ← glpR	3,560,455	+G
C_0, C_1, C_2, C_3, C_4, C_5	gltP → / ← yjcO	4,296,380	+CG

Evaluation
Probably ancestral
Control Adaptation
Control Unique
Adaptation Ag Resistant
Unique Ag resistant

Genomic variants were called in consensus mode; thus all have a frequency of 1.00 in their specific population. Mutation Description: Δ = deletion; i = insertion; ⇒ = point mutation

Table 6b. Genomic Variants (Annotation and Description) Control Populations, Generation 100

Gene	Annotation	Description
[crl]		[crl]
ybhI →	coding (933-941/1434 nt)	putative transporter
ychE → / → oppA	intergenic (+254/-485)	UPF0056 family inner membrane protein/oligopeptide transporter subunit
insB1–insA		insB1, insA
insA ← / → uspC	intergenic (-271/-264)	IS1 repressor TnpA/universal stress protein
gatC ←	pseudogene (1-2/442 nt)	pseudogene, galactitol-specific enzyme IIC component of PTS*
menC ←	coding (132-135/963 nt)	O-succinylbenzoyl-CoA synthase
rpoA ←	R191C (CGT→TGT)	RNA polymerase, alpha subunit
glpR ← / ← glpR	intergenic (-2/+1)	pseudogene, DNA-binding transcriptional repressor; regulator*
gltP → / ← yjcO	intergenic (+586/+56)	glutamate/aspartate:proton symporter/Sel1 family TPR-like repeat protein

*Abbreviated description, color scheme denote evaluations from Table 6a.

Table 7a. Genomic Variants in *E. coli* K12 MG1655 (Treatment Populations) Generation 100

Populations	Gene	Position	Mutation
T_1, T_2, T_3, T_4, T_5	[crl]	257,908	Δ776 bp
T_4	cusS ←	593,467	T→G
T_3	ychE → / → oppA	1,299,499	Δ1,199 bp
T_1, T_2, T_3, T_4	insB1–insA	1,978,503	Δ776 bp
T_1, T_2, T_3, T_5	insA ← / → uspC	1,979,486	IS5 (+) +4 bp
T_1, T_2, T_3, T_4, T_5	gatC ←	2,173,361	Δ2 bp
T_1, T_2, T_3, T_4, T_5	glpR ← / ← glpR	3,560,455	+CG
T_3	pyrE ← / ← rph	3,815,808	A→C
T_2, T_3, T_4, T_5	rpoB →	4,182,803	C→A
T_1, T_2, T_3, T_4, T_5	gltP → / ← yjcO	4,296,380	+CG

Evaluation
Probably ancestral
Control Adaptation
Control Unique
Adaptation Ag Resistant
Unique Ag resistant

Mutation Description: Δ = deletion; i = insertion; ➡ = point mutation

Table 7b. Genomic Variants (Annotation and Description) Treatment Populations, Generation 100

Gene	Annotation	Description
[crl]		[crl]
cusS ←	D435A (GAC→GCC)	sensory histidine kinase in two-component regulatory system with CusR, senses copper ions
ychE → / → oppA	intergenic (+254/-485)	UPF0056 family inner membrane protein/oligopeptide transporter subunit
insB1–insA		insB1, insA
insA ← / → uspC	intergenic (-271/-264)	IS1 repressor TnpA/universal stress protein
gatC ←	pseudogene (1-2/442 nt)	pseudogene, galactitol-specific enzyme IIC component of PTS*
glpR ← / ← glpR	intergenic (-2/+1)	pseudogene, DNA-binding transcriptional repressor;regulator*
pyrE ← / ← rph	intergenic (-40/+26)	orotate phosphoribosyltransferase/ribonuclease PH (defective)*
rpoB →	P520Q (CCG→CAG)	RNA polymerase, beta subunit
gltP → / ← yjcO	intergenic (+586/+56)	glutamate/aspartate:proton symporter/Sel1 family TPR-like repeat protein

Table 8a. Genomic Variants in *E. coli* K12 MG1655 (Control and Treatment Populations) Generation 150.

Populations	Gene	Pos.	Mutation
C_1, C_2, C_3, C_4, C_5, T_2, T_3, T_4	[crl]	257,906	Δ776 bp
C_3, C_4	cynR ←	357,104	T→C
C_0, C_4?	cynR ←	357,114	C→A
C_0?, C_1, C_2?, C_3?, C_4?, C_5?	yaiX ←	381,337	IS2 (–) +5 bp
C_1	insD1 →	382,113	IS2 (–) +5 bp
C0, C's and T's	ylbE →	547,694	A→G
C0, C's and T's	ylbE →	547,835	+G
T_3	cusS ←	592,690	T→G
T_3	cusS ←	593,467	T→G
C_0, C_2?, C_5?	insB1–insA	1,976,527	Δ776 bp
C_0, C_1, C_3, C_4	insA ← / → uspC	1,977,510	IS5 (+) +4 bp
C_2, C_3, T_4	insB1–insA	1,978,503	Δ776 bp
C_1, C_2, C_3, C_5, T_2, T_3, T_4	insA ← / → uspC	1,979,486	IS5 (+) +4 bp
T_1, C_2?	wbbK ←	2,102,274	G→A
T_1	wbbK ←	2,104,250	G→A
C_1, C_2 , C_3, C_4, C_5, T_1, T_2, T_3, T_4	gatC ←	2,173,361	Δ2 bp
T_3	purL ←	2,692,152	G→T
T_3	purL ←	2,694,130	G→T
T_3	ompR ←	3,534,074	Δ57 bp
T_3	ompR ←	3,536,052	Δ57 bp
C_1, C_2, C_3, C_4, C_5, T_1, T_2, T_3, T_4	glpR ← / ← glpR	3,560,455	+G
C_0, C_1, C_2, C_3, C_4, C_5	ppiC ← / ← yifN	3,957,957	C→T
C_3, C_4, C_5, T_3	rhaM ←	4,093,134	T→G
T_3	rpoB →	4,180,843	C→T
T_3	rpoB →	4,182,820	C→T
C_0, C_1, C_2, C_3, C_4, C_5	rpoC →	4,184,555	A→G
C_1, C_2, C_3, C_4, C_5, T_1, T_2, T_4	rpoC →	4,186,532	A→G
C_0, C_1, C_2, C_3, C_4, C_5	gltP → / ← yjcO	4,294,404	+GC
C_1, C_2, C_3, C_4, C_5, T_1, T_2, T_3, T_4	gltP → / ← yjcO	4,296,380	+CG
C_1	sgcR ←	4,526,151	IS5 (+) +4 bp
C_1, C_5, T_2	bglJ →	4,604,344	C→T
T_5	nadR → / ← yjjK	4,626,672	A→C

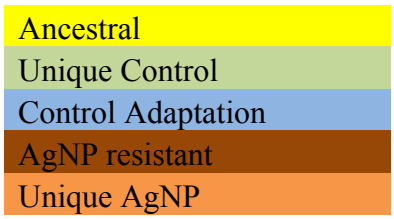

Mutation Description: Δ = deletion; i = insertion; ➡ = point mutation

Table 8b. Genomic Variants (Annotation and Description) Treatment and Control Populations, Generation 150.

Gene	Annotation	Description
[crl]		[crl]
cynR ←	K271E (AAA→GAA)	transcriptional activator of cyn operon; autorepressor
cynR ←	L267F (TTG→TTT)	transcriptional activator of cyn operon; autorepressor
yaiX ←	pseudogene (756-760/2029 nt)	pseudogene, interrupted by IS2A, acetyltransferase homolog; putative transferase; nonfunctional; interruped by IS2
insD1 →	coding (440-444/906 nt)	IS2 transposase TnpB
ylbE →	pseudogene (114/1259 nt)	putative protein, C-ter fragment (pseudogene)
ylbE →	pseudogene (255/1259 nt)	putative protein, C-ter fragment (pseudogene)
cusS ←	D435A (GAC→GCC)	sensory histidine kinase in two-component regulatory system with CusR, senses copper ions
cusS ←	D435A (GAC→GCC)	sensory histidine kinase in two-component regulatory system with CusR, senses copper ions
insB1–insA		insB1, insA
insA ← / → uspC	intergenic (-271/-264)	IS1 repressor TnpA/universal stress protein
insB1–insA		insB1, insA
insA ← / → uspC	intergenic (-271/-264)	IS1 repressor TnpA/universal stress protein
wbbK ←	T87M (ACG→ATG)	lipopolysaccharide biosynthesis protein
wbbK ←	T87M (ACG→ATG)	lipopolysaccharide biosynthesis protein
gatC ←	pseudogene (1-2/442 nt)	pseudogene, galactitol-specific enzyme IIC component of PTS;transport; Transport of small molecules: Carbohydrates, organic acids, alcohols; PTS system galactitol-specific enzyme IIC
purL ←	R472S (CGC→AGC)	phosphoribosylformyl-glycineamide synthetase

purL ←	R472S (CGC→AGC)	phosphoribosylformyl-glycineamide synthetase
ompR ←	coding (477-533/720 nt)	DNA-binding response regulator in two-component regulatory system with EnvZ
ompR ←	coding (477-533/720 nt)	response regulator in two-component regulatory system with EnvZ
glpR ← / ← glpR	intergenic (-2/+1)	pseudogene, DNA-binding transcriptional repressor;regulator; Energy metabolism, carbon: Anaerobic respiration; repressor of the glp operon/pseudogene, DNA-binding transcriptional repressor;regulator; Energy metabolism, carbon: Anaerobic respiration; repressor of the glp operon
ppiC ← / ← yifN	intergenic (-121/+78)	peptidyl-prolyl cis-trans isomerase C (rotamase C)/conserved protein (pseudogene)
rhaM ←	Y102S (TAC→TCC)	L-rhamnose mutarotase
rpoB →	H526Y (CAC→TAC)	RNA polymerase, beta subunit
rpoB →	H526Y (CAC→TAC)	RNA polymerase, beta subunit
rpoC →	K395E (AAA→GAA)	RNA polymerase, beta prime subunit
rpoC →	K395E (AAA→GAA)	RNA polymerase, beta prime subunit
gltP → / ← yjcO	intergenic (+587/+55)	glutamate/aspartate:proton symporter/hypothetical protein
gltP → / ← yjcO	intergenic (+586/+56)	glutamate/aspartate:proton symporter/Sel1 family TPR-like repeat protein
sgcR ←	coding (735-738/783 nt)	putative DNA-binding transcriptional regulator
bglJ →	S62F (TCT→TTT)	bgl operon transcriptional activator
nadR → / ← yjjK	intergenic (+102/+206)	trifunctional protein: nicotinamide mononucleotide adenylyltransferase, ribosylnicotinamide kinase, transcriptional repressor/fused predicted transporter subunits of ABC superfamily: ATP-binding components

Table 9a. Genomic Variants in *E. coli* K12 MG1655 (Control and Treatment Populations) Generation 200.

Stock	Gene	Pos.	Mutation
C_0, C_1, C_3, C_4, C_5, T_1, T_2, T_5	[crl]	257,908	Δ776 bp
T_4	allR → / → gcl	533,893	C→A
T_1, T_2, T_3, T_4, T_5	cusS ←	593,467	T→G
C_2, C_4, C_5, T_2, T_5	ychE → / → oppA	1,299,499	Δ1,199 bp
C_1, C_4, C_5, T_1, T_2, T_4, T_5	insB1–insA	1,978,503	Δ776 bp
C_1, C_2, C_3, C_4, C_5, T_1, T_2, T_4, T_5	insA ← / → uspC	1,979,486	IS5 (+) +4 bp
C_0, C_1, C_2, C_3, C_4, C_5, T_1, T_2, T_3, T_4, T_5	gatC ←	2,173,361	Δ2 bp
C_2	ccmE ←	2,295,168	C→T
T_1, T_2, T_4, T_5	purL ←	2,694,130	G→T
C_1	rpoA ←	3,440,459	G→A
T_1	ompR ←	3,536,264	Δ1 bp
T_2	ompR ←	3,536,342	Δ12 bp
T_5	ompR ←	3,536,570	IS3 (–) +4 bp :: +TCA
C_0, C_1, C_2, C_3, C_4, C_5, T_1, T_2, T_3, T_4, T_5	glpR ← / ← glpR	3,560,455	+G
T_1, T_2, T_3, T_4, T_5	rpoB →	4,182,820	C→T
C_2, C_3, C_4, C_5	rpoC →	4,186,532	A→G
C_0, C_1, C_2, C_3, C_4, C_5, T_1, T_2, T_4, T_5	gltP → / ← yjcO	4,296,380	+CG

Mutation Description: Δ = deletion; i = insertion; ⟶ = point mutation

Table 9b. Genomic Variants (Annotation and Description) Treatment and Control Populations, Generation 200

Gene	Annotation	Description
[crl]		[crl]
allR → / → gcl	intergenic (+67/-23)	transcriptional repressor of all and gcl operons; glyoxylate-induced/glyoxylate carboligase
cusS ←	D435A (GAC→GCC)	sensory histidine kinase in two-component regulatory system with CusR, senses copper ions
ychE → / → oppA	intergenic (+254/-485)	UPF0056 family inner membrane protein/oligopeptide transporter subunit
insB1–insA		insB1, insA
insA ← / → uspC	intergenic (-271/-264)	IS1 repressor TnpA/universal stress protein
gatC ←	pseudogene (1-2/442 nt)	pseudogene, galactitol-specific enzyme IIC component of PTS;transport*
ccmE ←	V71V (GTG→GTA)	periplasmic heme chaperone
purL ←	R472S (CGC→AGC)	phosphoribosylformyl-glycineamide synthetase
rpoA ←	R191C (CGT→TGT)	RNA polymerase, alpha subunit
ompR ←	coding (321/720 nt)	response regulator in two-component regulatory system with EnvZ
ompR ←	coding (232-243/720 nt)	response regulator in two-component regulatory system with EnvZ
ompR ←	coding (12-15/720 nt)	response regulator in two-component regulatory system with EnvZ
glpR ← / ← glpR	intergenic (-2/+1)	pseudogene, DNA-binding transcriptional repressor;regulator; Energy metabolism*
rpoB →	H526Y (CAC→TAC)	RNA polymerase, beta subunit
rpoC →	K395E (AAA→GAA)	RNA polymerase, beta prime subunit

gltP → / ← yjcO	intergenic (+586/+56)	glutamate/aspartate:proton symporter/Sel1 family TPR-like repeat protein

Yellow - Ancestral shared

Light Blue - Control specific

Blue -- Control Adaptation

Light Orange - Evolved AgNP specific

Orange - Evolved AgNP shared

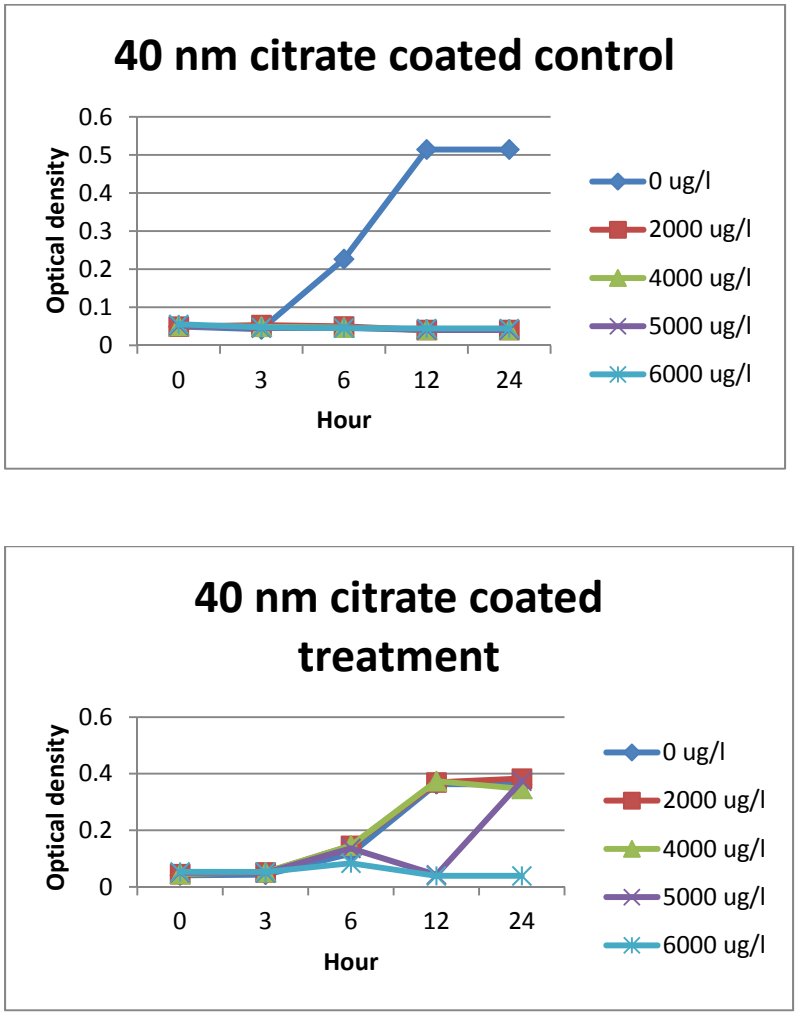

Figure 1. Population Growth as Measured by Optical Density of the Treatment and Control Bacterial Cocktails at Generation 250 Exposed to 40nm Citrate-Coated Silver Nanoparticles.

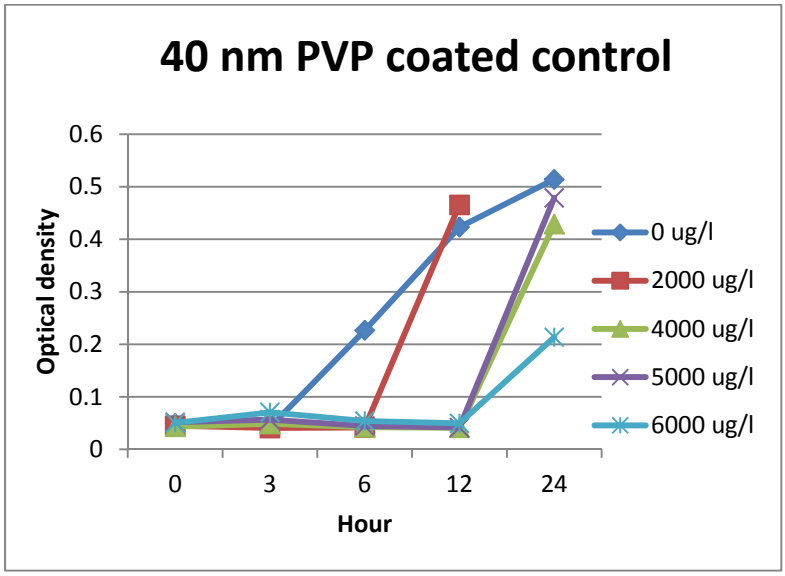

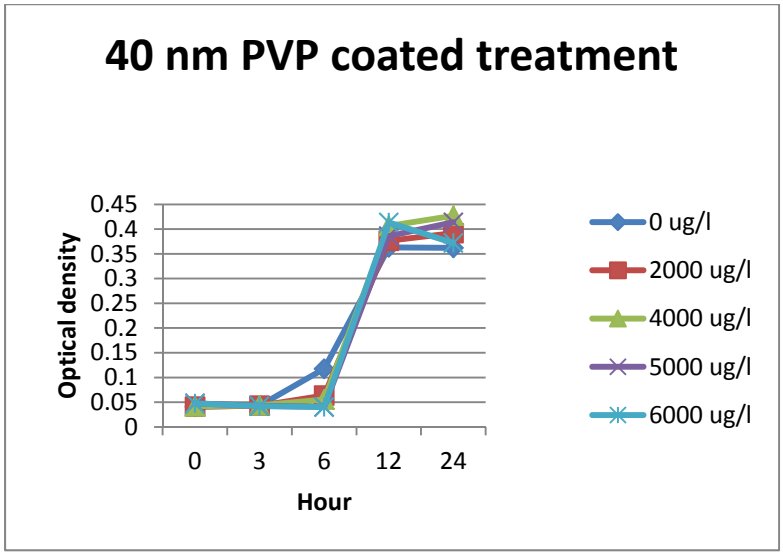

Figure 2. Population Growth as Measured by Optical Density of the Treatment and Control Bacterial Cocktails at 250 Generations Exposed to 40nm PVP-Coated Silver Nanoparticles.

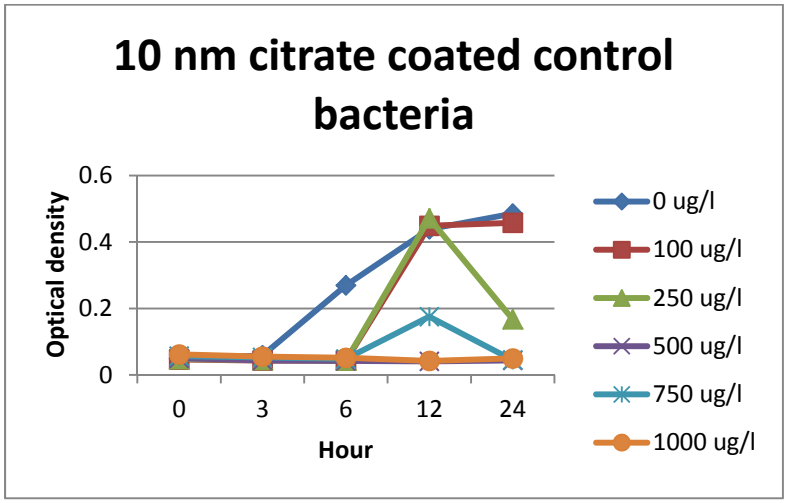

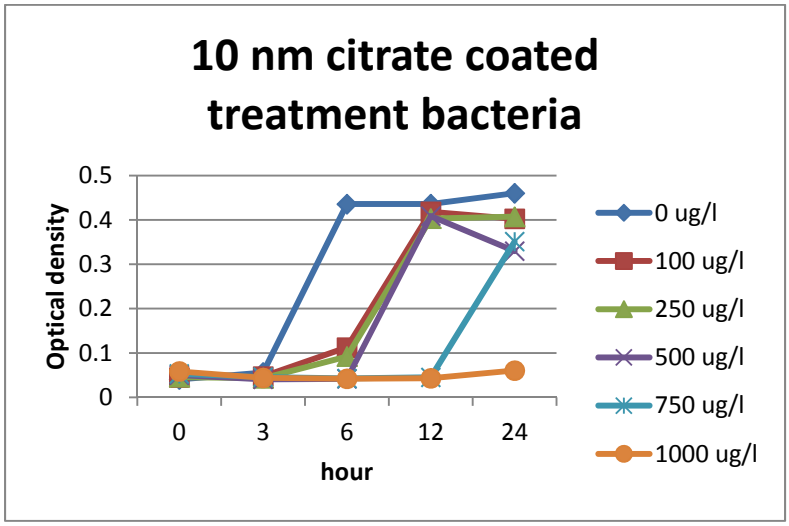

Figure 3. Population Growth of Control and Treatment Cocktails as Measured by Optical Density of Bacteria Exposed to Different Concentrations of 10 nm Citrate Coated Silver Nanoparticles at 250 Generations.

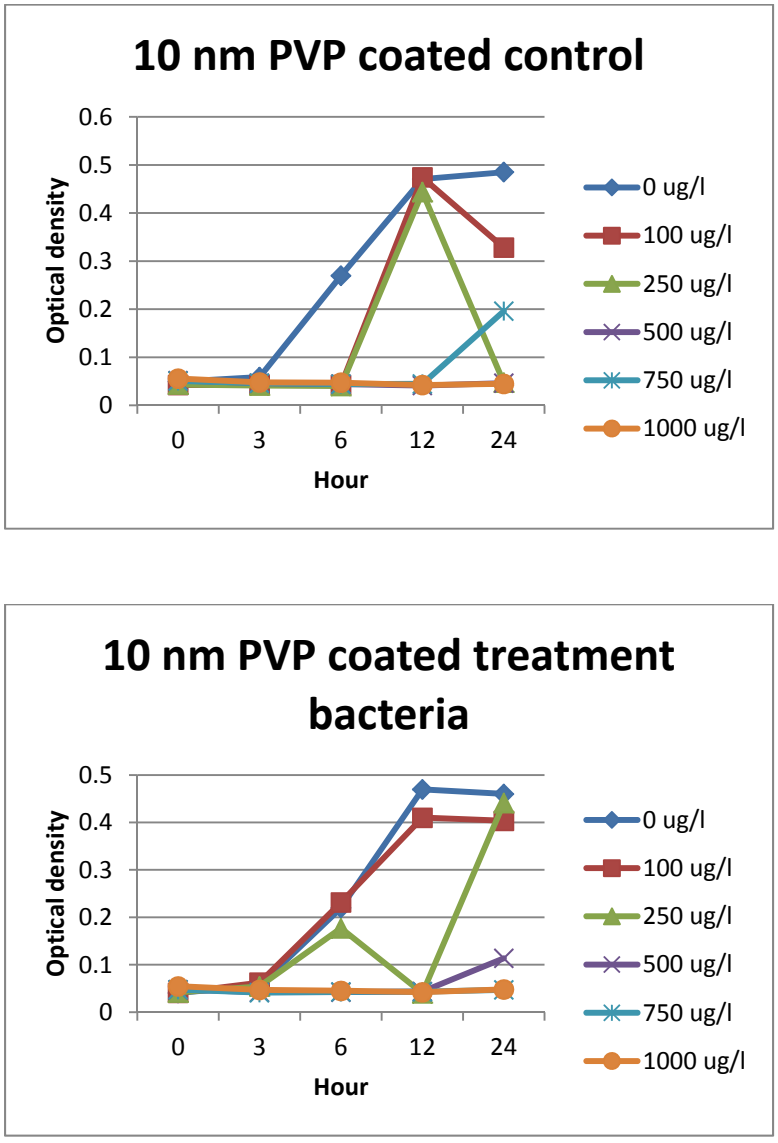

Figure 4. Population Growth of Control and Treatment Bacterial Cocktails as Measured by Optical Density of Treatment and Control Bacteria at Generation 250 Exposed to 10nm PVP-Coated Silver Nanoparticles.

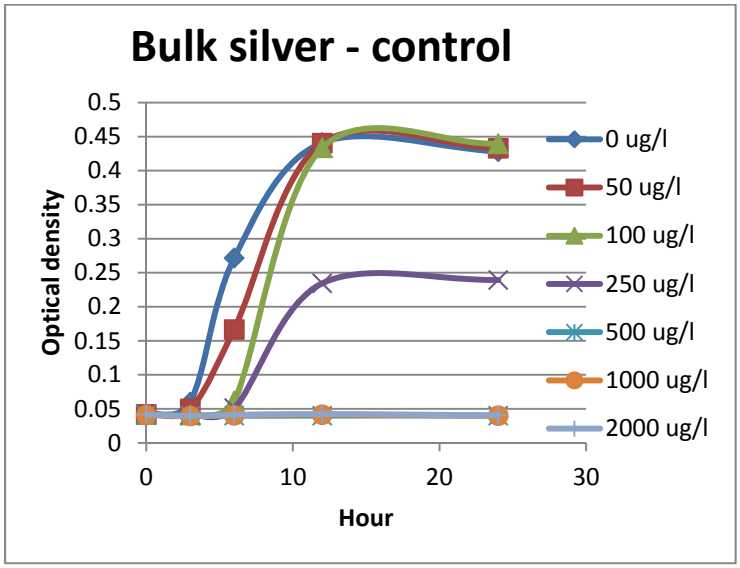

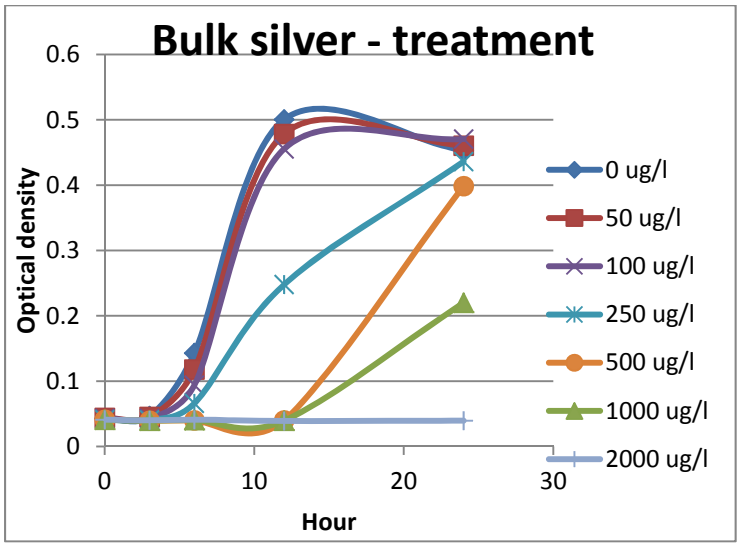

Figure 5. Population Growth of Control and Treatment Bacterial Cocktails as Measured by Optical Density of the Treatment and Control Bacteria at Generation 250 Exposed to Bulk Silver Nitrate.

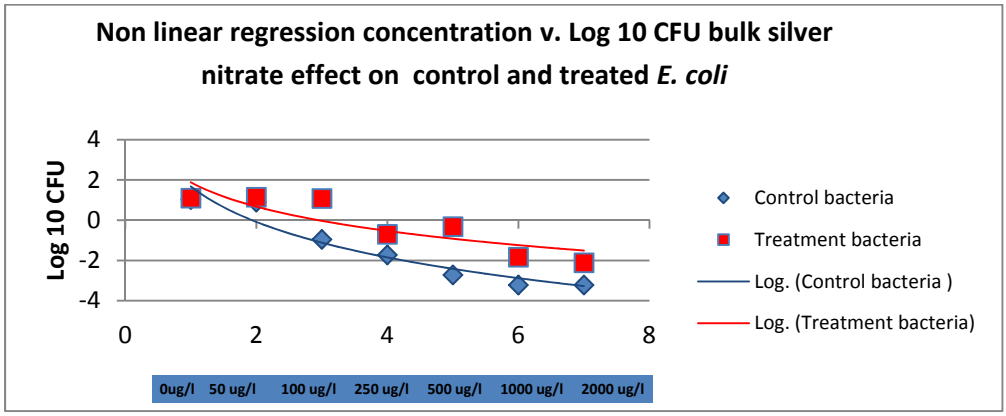

Figure 6a. Difference in Colony Forming Units (log 10 CFU) for Treatment and Control Bacteria at Generation 305 Exposed to Different Concentrations of Bulk Silver ($AgNO_3$) over 24 Hours.

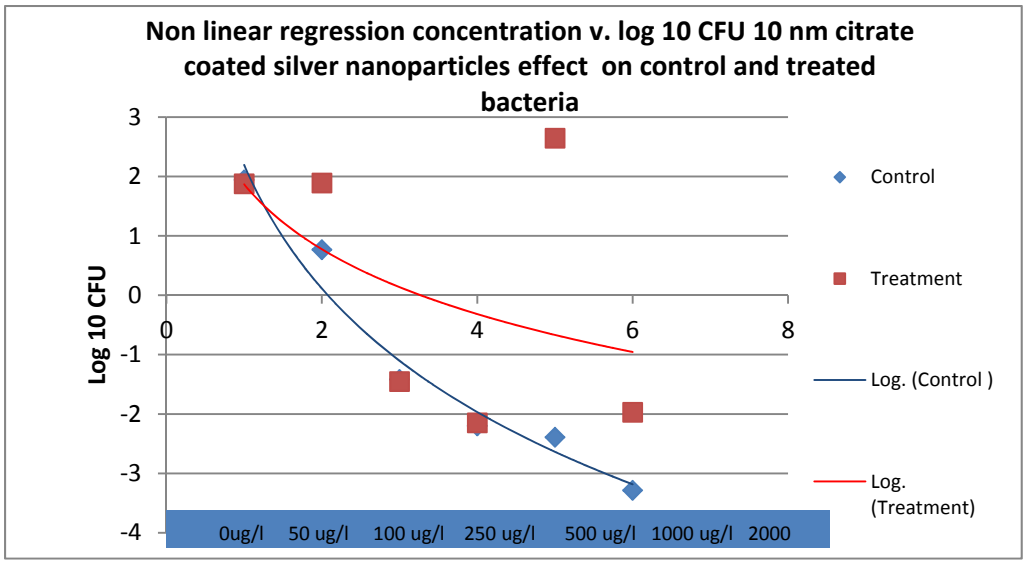

Figure 6b. Difference in Colony Forming Units (log 10 FU) for Treatment and Control Bacteria at Generation 305 Exposed to Different Concentrations of 10 nm Citrate Coated Silver Nanoparticles for 24 Hours.

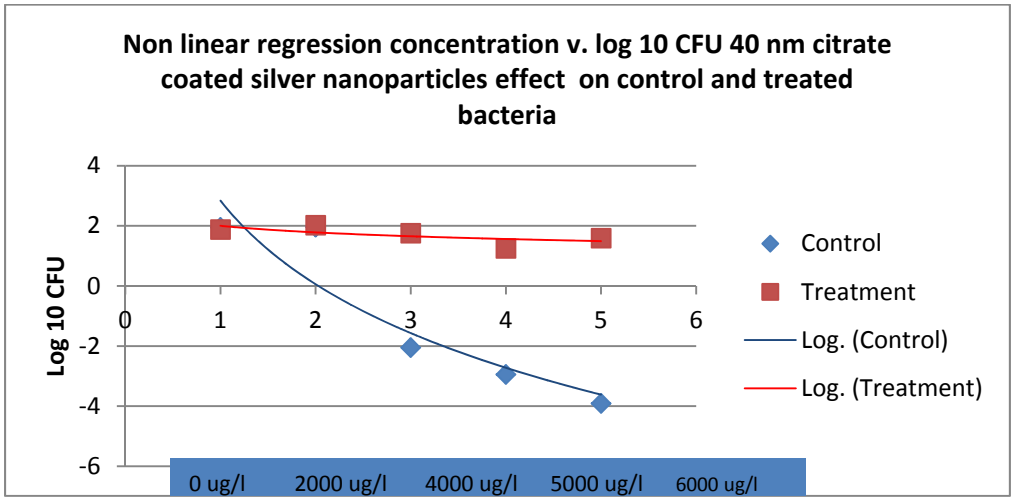

Figure 6c. Difference in Colony Forming Units (log 10 CFU) for Treatment and Control Bacteria at Generation 305 Exposed to Different Concentrations of 40 nm Citrate Coated Silver Nanoparticles for 24 Hours.

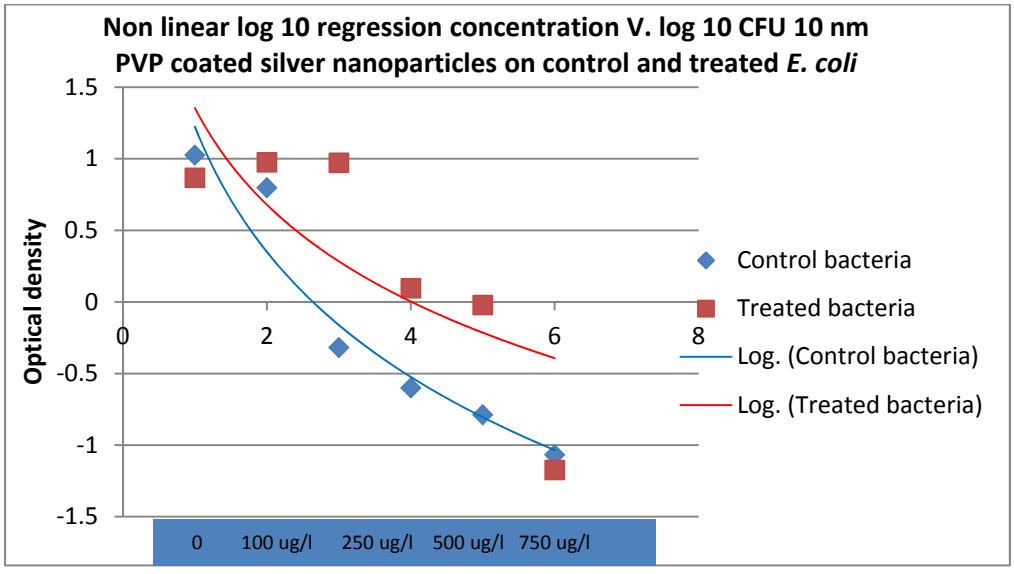

Figure 6d. Difference in Colony Forming Units (log 10 CFU) for Treatment and Control Bacteria at Generation 305 Exposed to Different Concentrations of 10 nm PVP-Coated Silver Nanoparticles for 24 Hours.

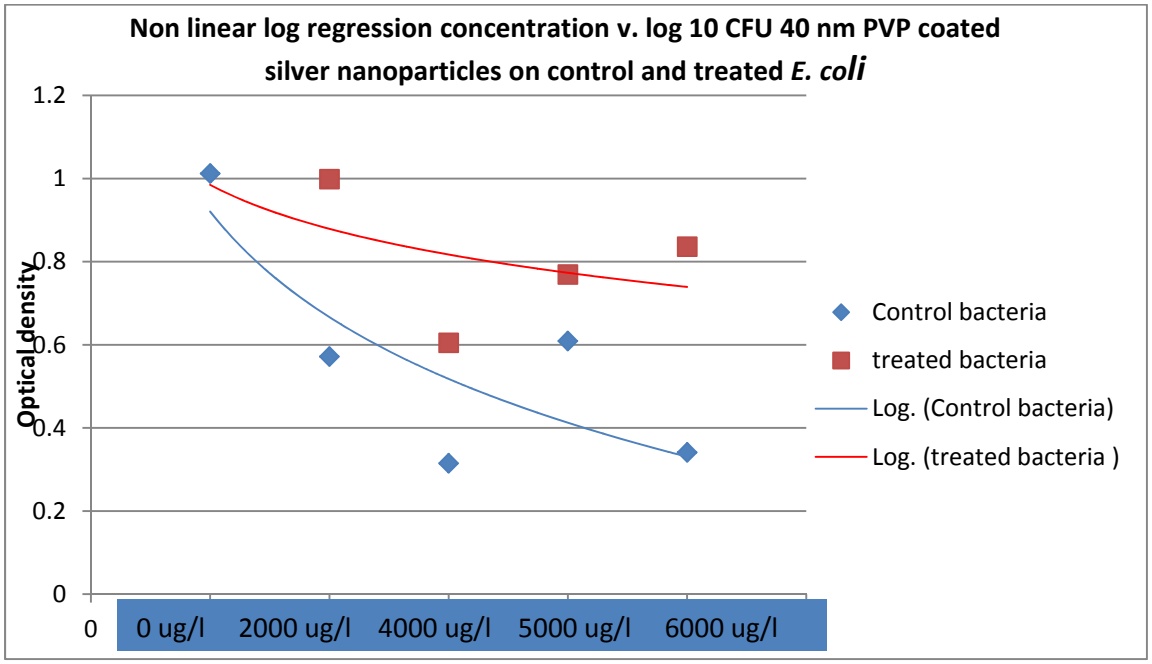

Figure 6e. Difference in Colony Forming Units (log 10 CFU) for Treatment and Control Bacteria at Generation 305 Exposed to Different Concentrations of 40 nm PVP-Coated Silver Nanoparticles for 24 Hours.

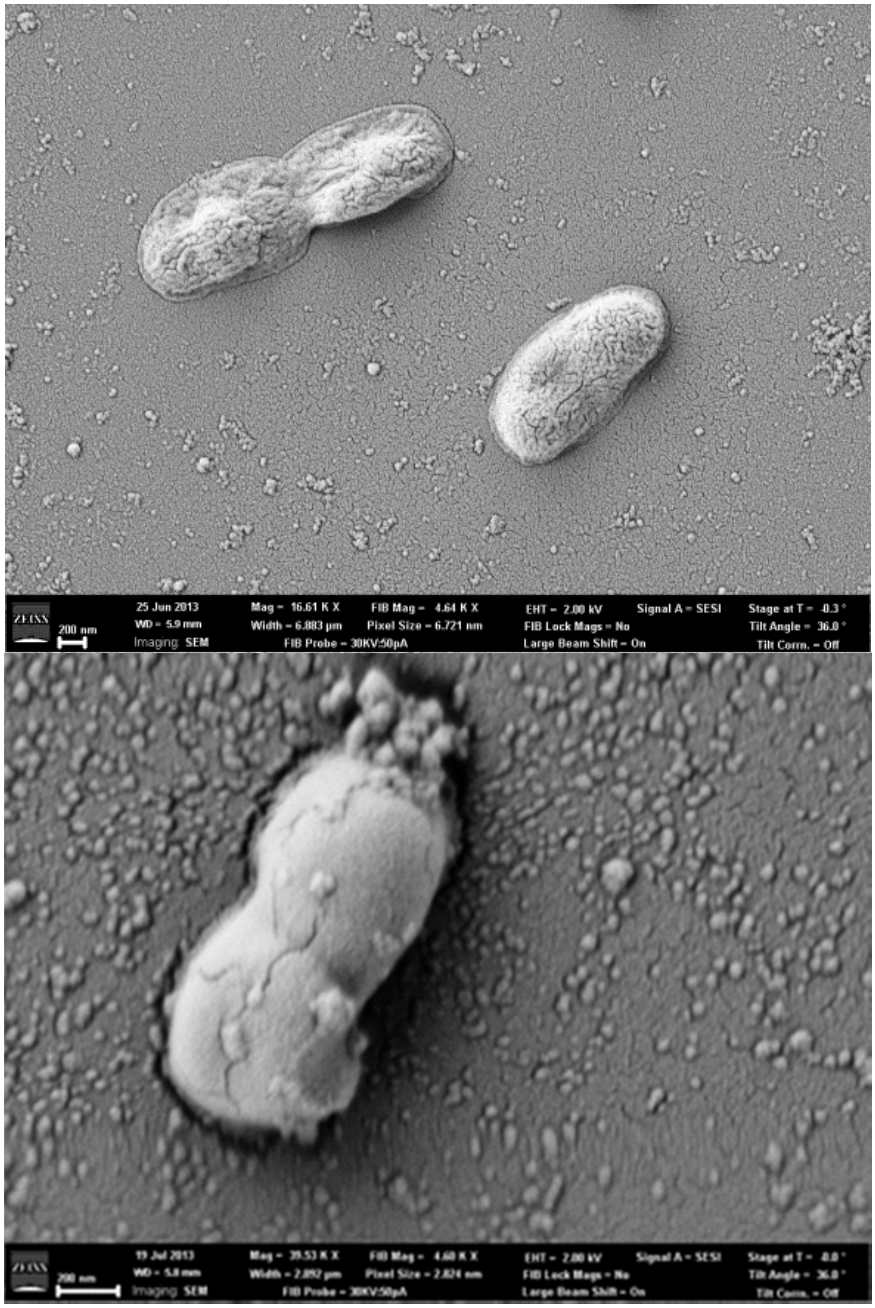

Figure 7. SEM Images of *E. coli* MG1655 (a) No AgNPs were added to this Preparation (b) Treated with 20 µg/L40 nm PVP-Coated Spherical Silver Nanoparticles.

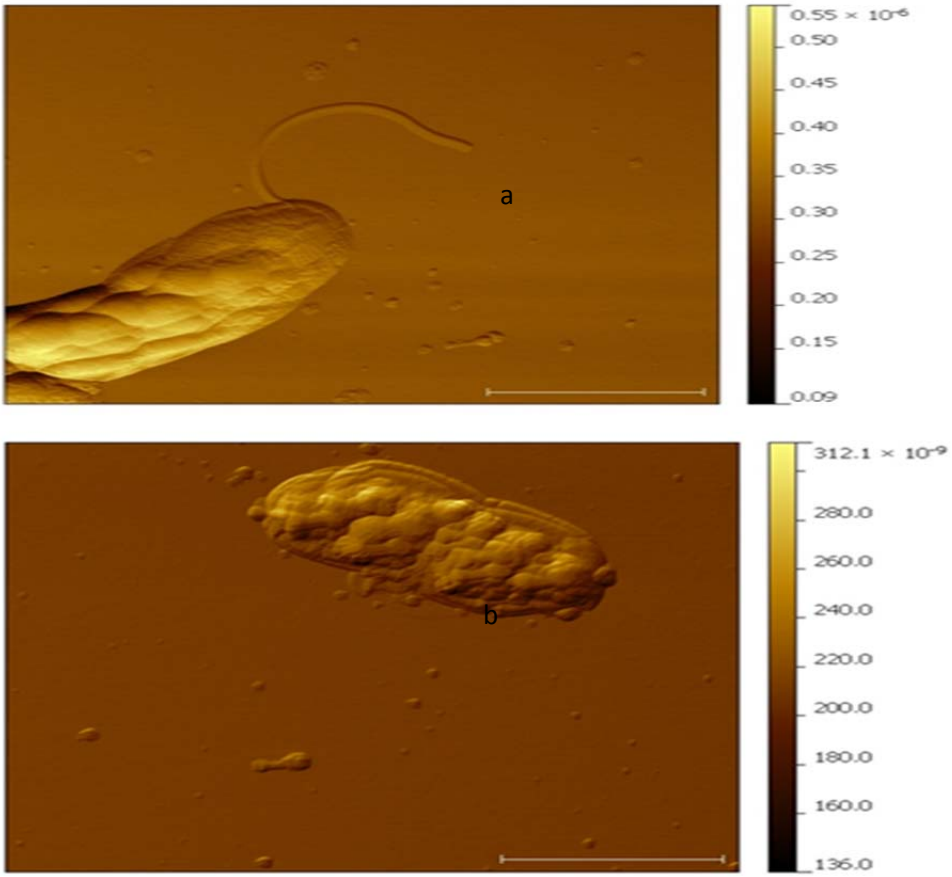

Figure 8. AFM Images of *E. coli* MG1655 at Generation 250 (a) Control (b) Treatment with 250 µg/l 10 nm Citrate-Coated Spherical Silver Nanoparticles.

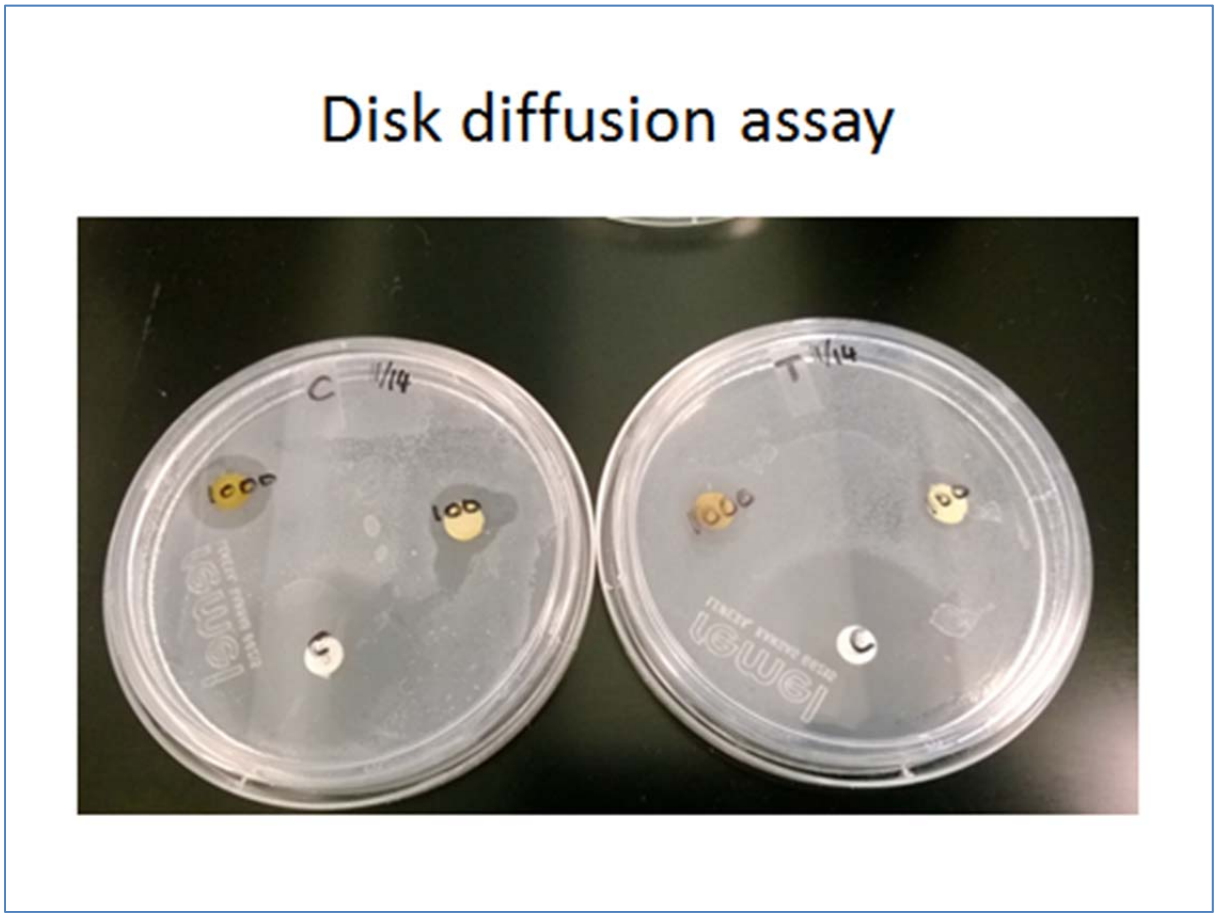

Figure 9. Disc Diffusion Assay to Determine Differences between Control (a) Treatment Populations (b) of *E. coli* K-12 at 250 Generations.

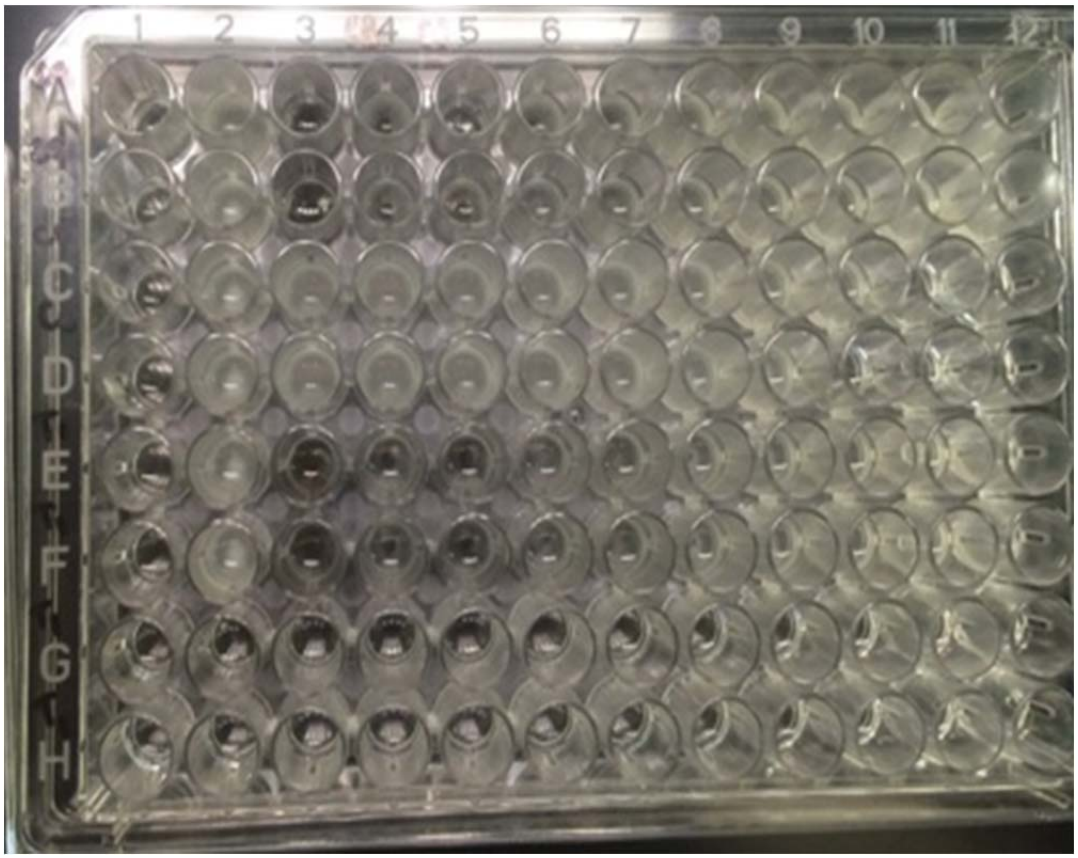

Figure 10. Micro dilution Result of 40nm Citrate Coated to Determine Differences between Treated (lines EFGH) and Non-Treated (lines ABCD)